Carbon Through a Restored Salt Marsh: Organic Matter Sources and Greenhouse Gas Fluxes Across an Elevation Gradient

by

Kristine Bolibol Bernabe

A thesis accepted and approved in partial fulfillment of the

requirements for the degree of

Master of Science

in Biology

Thesis Committee:

Lillian Aoki, Chair

Karen Adair, Member

Lucas Silva, Member

University of Oregon

Summer 2026

© 2026 Kristine Bolibol Bernabe

THESIS ABSTRACT

Kristine Bolibol Bernabe

Master of Science in Biology

Title: Carbon Through a Restored Salt Marsh: Organic Matter Sources and Greenhouse Gas Fluxes Across an Elevation Gradient

Restored tidal salt marshes are increasingly recognized as blue carbon ecosystems with potential to sequester carbon and mitigate climate change, yet the carbon dynamics of restored marshes remain poorly characterized, particularly in the Pacific Northwest. This thesis examined the composition of organic matter sources and greenhouse gas flux dynamics across an elevation gradient in Kunz Marsh, a restored tidal salt marsh within the South Slough National Estuarine Research Reserve in Coos Bay, Oregon. Using stable isotope analysis and Bayesian mixing models, organic matter source composition was found to vary systematically with elevation: salt marsh-derived carbon dominated across all elevation zones but decreased with elevation, terrestrial contributions increased with elevation, and estuarine contributions remained low throughout but peaked in the low marsh. Despite sharing the same elevation, the restored high marsh differed from an adjacent reference high marsh in carbon source composition, suggesting that full recovery toward reference conditions has not yet occurred after nearly 30 years of restoration. Greenhouse gas flux analysis revealed that elevation was not a significant predictor of CO_2 or CH_4 flux. Instead, seasonal CO_2 flux responded to photosynthetically active radiation and air temperature, while CH_4 flux was primarily governed by vegetation-mediated transport, with Normalized Difference Vegetation Index (NDVI), a proxy for vegetation density, as the only significant predictor. Kunz Marsh was a consistent net source of both gases across sampling dates, highlighting the complexity of evaluating the restoration of tidal marshes as a climate mitigation strategy and the need for long-term carbon monitoring in restored systems.

ACKNOWLEDGMENTS

This work would not have been possible without the help of many people and groups. I will try my absolute best to thank them within this small space, although I acknowledge that there are not enough words to express my gratitude to each of them fully.

First, I express overwhelming gratitude to my advisor, Dr. Lillian Aoki, for her unending support throughout this research project. Thank you for taking a chance on me two years ago by accepting me into your lab and seeing my eagerness to be a scientist. Thank you for helping me work through every detail of this work and giving me the support and freedom to pursue my interests in ecosystem science, and for introducing me to coastal wetlands, a forever icon in my career as an ecologist.

Thank you to my other committee members, Dr. Karen Adair and Dr. Lucas Silva, for their extended support with this project. To Karen, for helping me navigate the challenges of working in a wet lab, and to Lucas for supporting all things carbon research. Thank you to everyone involved with CARBS for supporting this work and inspiring me to consider new questions about carbon dynamics across Oregon. Thank you to the South Slough Reserve staff, especially Jennifer Kirkland, for their support with the logistics of this project and for providing vegetation data and drone imagery. Your commitment to helping scientists study these wetland systems, especially during such a tumultuous time for science, is admirable.

A special thank you goes out to my labmates: Kate Kelly, Mara Salisbury, Katya Podkovyroff, and Rachael Dennis. Thank you for all your help in and out of the field. You helped me keep my sanity during the past two years and have truly made graduate school such a memorable experience. Thank you to my undergraduate Ezra Bergson-Michelson for helping me

with every single one of my sampling days. The data would be nonexistent without you. I wish you endless success in your scientific career; any graduate program would be lucky to have you.

Lastly, thank you to all my friends and family who have been with me at every step. To my mom and dad, thank you for all the sacrifices you have made to provide me with these opportunities. To my siblings, Michael, John, Luigie, Luckie, and Gheeriel, thank you for making life such chaotic fun. To our family dog, June, thank you for being you. To friends and family from San Diego (DeeDee, Danielle, Francia, Kyle), Hawaii, and the Philippines, who have shaped who I am today and motivated me to pursue graduate school, I thank you deeply. To friends in Oregon, thank you for sharing this journey with me and being a support system in a new place. To Zac, my partner, thank you for being by my side through all of it. Your support means the world to me. You have made Eugene feel like home.

I am eternally grateful to every single one of you.

TABLE OF CONTENTS

Chapter Page

I. LIST OF FIGURES 8

II. LIST OF TABLES 9

III. GENERAL INTRODUCTION 10

IV. CARBON SOURCES ACROSS A SALT MARSH ELEVATION GRADIENT: A STABLE ISOTOPE APPROACH 12

Introduction 12

Methods 16

Site Description 16

Soil Core Sampling Design 18

Isotope Analysis ($\delta^{13}C$, $\delta^{15}N$) 19

Statistical Analysis 20

Results 21

$\delta^{13}C$ Versus $\delta^{15}N$ 21

Carbon Sources 23

Discussion 27

Conclusion 32

V. GREENHOUSE GAS FLUX DYNAMICS ACROSS A SALT MARSH ELEVATION GRADIENT 35

Introduction 35

Methods 38

Site Description 38

Seasonal Greenhouse Gas Flux Sampling 40
Diel Greenhouse Gas Flux Sampling 41
Environmental Covariates 41
Statistical Analyses 44
Seasonal Flux Models 44
Diel Flux Models 45
Results 46
Seasonal Carbon Dioxide Flux 46
Seasonal Methane Flux 47
Diel Flux Dynamics for Carbon Dioxide and Methane 49
Discussion 53
Conclusion 60
VI. GENERAL CONCLUSION 64
APPENDIX: SUPPLEMENTAL FIGURES AND TABLES 66
REFERENCES CITED 69

I. LIST OF FIGURES

Figure Page

1.1 Orthomosaic imagery of Kunz Marsh and Tom's Creek Marsh within the South Slough National Estuarine Research Reserve 18

1.2 Stable isotope biplot of $\delta^{13}C$ and $\delta^{15}N$ values (‰) for surface sediment samples collected across three elevation zones at Kunz Marsh at Tom's Marsh 22

1.3 Posterior probability density distributions of organic matter source contributions (%) estimated by mixSIAR for each site: Kunz Low (KL), Kunz Mid (KM), Kunz High (KH), and Tom's Marsh reference site (TMR)..... 25

1.4 Posterior distributions of organic matter source contributions (%) estimated by MixSIAR for each site across estuarine, salt marsh, and terrestrial sources 26

2.1 Drone orthomosaic imagery of Kunz Marsh within the South Slough National Estuarine Research Reserve 39

2.2 Relationships between greenhouse gas fluxes and environmental predictors (A) and marsh surface elevation (B) across nine collars (low marsh: LM1-LM3; mid marsh: MM1-MM3; high marsh: HM1-HM3) 49

2.3 Diel patterns in CH_4 and CO_2 flux (µmol m^{-2} min^{-1}) measured across four high marsh collars (HM1-HM4) during the 24-hour sampling campaign 50

2.4 Greenhouse gas flux measurements from the 24-hour sampling campaign 51

2.5 Relationships between CO_2 flux (µmol m^{-2} min^{-1}) and environmental predictors during dark (A) and light (B) periods measured across the high marsh during the Kunz Marsh 24-hour sampling campaign..... 52

2.6 Relationships between CH_4 flux (µmol m^{-2} min^{-1}) and environmental predictors during dark (A) and light (B) periods measured across the high marsh during the Kunz Marsh 24-hour sampling campaign..... 53

S1 Vegetation composition across low, mid, and high elevation zones at Kunz Marsh based on 2023 point-intercept survey data collected by South Slough National Estuarine Research Reserve 68

II. LIST OF TABLES

Table Page

1.1 Dunn's pairwise comparisons of $\delta^{13}C$ and $\delta^{15}N$ values among elevation zones at Kunz Marsh and Tom's Marsh reference site 22

1.2 MixSIAR posterior estimates of organic matter source contributions for each site 23

2.1 Linear mixed model results for CO_2 flux (μmol m^{-2} min^{-1}). 46

2.2 Generalized additive mixed model results for CH_4 flux (log-transformed; μmol m^{-2} min^{-1}) 47

S1 GPS coordinates and surface elevations for all flux measurement collars at Kunz Marsh. 67

III. GENERAL INTRODUCTION

Blue carbon ecosystems, including coastal wetlands like salt marshes, are recognized for sequestering large amounts of carbon (Arias-Ortiz et al. 2024). This storage capacity is largely due to their high productivity, while environmental conditions such as frequent inundation and increased salinity slow or prevent decomposition (Chmura et al. 2003). As such, coastal wetlands are traditionally considered carbon sinks that support climate change mitigation (Hao et al. 2024). However, coastal wetlands have been extensively lost in some areas, including the Pacific Northwest. Oregon, specifically, has lost 58.9% of its historical tidal marshes (Brophy et al. 2019). Given the carbon storage benefits of wetlands and their extensive losses, restoration of coastal wetlands has increasingly been recognized as a nature-based climate solution (O'Connor et al. 2019). The goal is to restore these wetlands to recover the structure and function of reference, or undisturbed, marshes (Craft 2022), with the added benefit of restoring their carbon storage capacity, making these coastal wetlands potential climate change mitigation tools (Hao et al. 2024).

Realizing this restoration potential, however, requires a clearer understanding of the carbon dynamics that govern whether a restored marsh functions as a net carbon sink or source. Characterizing the origin of stored carbon is important because different organic matter pools reflect how carbon moves through the system and the marsh's biogeochemical character during restoration recovery (Drexler et al. 2020, Janousek et al. 2025). While coastal wetlands can sequester large quantities of carbon across different organic matter pools (Kauffman et al. 2020), carbon can also be lost from the system, specifically as greenhouse gas emissions. The same environmental conditions that slow down decomposition facilitate the production and release of CH_4, a potent greenhouse gas, into the atmosphere (IPCC 2023). These competing processes

emphasize the carbon source-sink tension in coastal wetlands (Arias-Ortiz et al. 2024). Carbon dynamics within coastal wetlands are further complicated by restoration, which can alter hydrology, vegetation communities, microbial communities, and organic matter pools (Drexler et al. 2020). All these factors can influence the net climate forcing of a restored wetland as it recovers toward reference marsh conditions, over timescales that remain poorly characterized (O'Connor et al. 2019). This thesis addresses these gaps by characterizing both organic matter source composition and CO_2 and CH_4 gas fluxes at Kunz Marsh, capturing carbon inputs and outputs, within a single restored marsh system. Kunz Marsh, a previously diked Oregon salt marsh restored through an experimental elevation manipulation, provides a unique opportunity to examine how elevation and restoration history jointly structure carbon dynamics (Cornu and Sadro 2002, Schultz et al. 2023). Compared with Washington and California, organic matter sources and greenhouse gas dynamics in Oregon salt marshes remain less well characterized (Schultz et al. 2023, Williams et al. 2025), and expanding this regional baseline knowledge is important for informed blue carbon accounting and restoration investment decisions across the Pacific Northwest (Janousek et al. 2025). By contributing to this regional baseline, this research has broader implications for wetland restoration investment and carbon offset markets in similar coastal systems (Hao et al. 2024).

IV. CARBON SOURCES ACROSS A SALT MARSH ELEVATION GRADIENT: A STABLE ISOTOPE APPROACH

Introduction

Coastal wetlands, such as tidal salt marshes, provide critical ecosystem functions, including carbon storage, making them important for climate change mitigation (Hao et al. 2024). Specifically, coastal wetlands store substantial amounts of blue carbon, which is organic matter (OM) that decomposes slowly in waterlogged soils, thereby remaining stored for centuries to millennia (Chmura et al. 2003). Blue carbon ecosystems sequester carbon at about 40 times the efficiency of terrestrial forests due to their anoxic, high-salinity sediments, which slow the mineralization of carbon and methanogenesis (O'Connor et al. 2019). This capacity to remove carbon from the atmosphere for long-term storage makes coastal wetlands relevant for climate change mitigation, carbon accounting frameworks, and wetland restoration planning (Hao et al. 2024).

However, the capacity of coastal wetlands to sequester carbon depends not only on how much OM accumulates, but also on where that OM originates. Carbon within coastal wetlands is stored primarily in soil and sediment, occurring as either autochthonous (in situ biological productivity) or allochthonous (terrestrial or marine sources) (Hao et al. 2024). The origin of soil organic carbon (SOC) matters for understanding tidal wetlands as carbon sinks, since whether carbon is autochthonous or transported has implications for the permanence of carbon within wetland soils and the true role of wetlands in carbon cycling (Janousek et al. 2025b). Given this, there are ongoing debates about whether allochthonous carbon should be included in carbon accounting for climate mitigation purposes. Interestingly, in a study about the spatiotemporal controls on OM sourcing in salt marshes, Peck et al. (2025) argued that not all buried carbon

contributes equally to climate mitigation, as petrogenic terrestrial OM may not represent recently fixed atmospheric CO_2 and therefore may not count toward genuine climate mitigation (Peck et al. 2025). At the same time, Drexler et al. (2020), in a study about carbon origin in restored and reference marshes, caution that allochthonous carbon should not be excluded from carbon accounting, as it comprises a substantial portion of the sediment carbon sink in both restored and reference marshes. Together, these ideas highlight that understanding the origin of wetland carbon, in addition to quantity, is essential to characterize the climate role of coastal wetlands accurately.

Stable isotopes are a well-established method to trace OM origins. $\delta^{13}C$ helps distinguish vegetation by indicating which photosynthetic pathway plants use. Within wetlands specifically, C3 plants typically range from -20 to -34‰ and C4 plants typically from -16 to -19‰ (Craft et al. 1988). $\delta^{13}C$ values also remain relatively stable throughout diagenesis, making them reliable tracers because they are not significantly affected by post-depositional processes. Combining $\delta^{13}C$ with $\delta^{15}N$ further improves carbon source partitioning by indicating whether material is from terrestrial, emergent marsh, or aquatic vegetation when carbon signatures alone are ambiguous (Craft et al. 1988). The inclusion of $\delta^{15}N$ signals the extent of nitrogen cycling and microbial processing within the system, as processes such as denitrification fractionate nitrogen isotopes and enrich residual substrate in ^{15}N. However, the direction and magnitude of enrichment depend on the rate and completeness of nitrogen transformation (Högberg 1997, Mariotti et al. 1982). $\delta^{13}C$ and $\delta^{15}N$ isotopes have been used in previous studies within the Pacific Northwest (PNW) to determine carbon sources within coastal wetlands. Kemp et al. (2010) used $\delta^{13}C$ and C:N ratios to reconstruct relative sea level rise by exploiting the elevational zonation of C3 and C4 plants based on salinity gradients. Drexler et al. (2020) used a Bayesian stable isotope

mixing model to partition organic carbon sources in marsh sediments based on $\delta^{13}C$, $\delta^{15}N$, and $\delta^{34}S$ across salinity gradients. However, these stable isotope mixing models have some limitations, including source-number constraints, end-member heterogeneity, and diagenetic fractionation between sources and samples (Craven et al. 2017). Despite these limitations, stable isotope tracers remain the standard approach for OM source partitioning within wetland soils, and efforts to further refine these models continue. Bayesian stable isotope mixing models, such as MixSIAR (Stock et al. 2018), represent such methodological progress in source partitioning by incorporating fixed and random effects and model selection criteria.

In addition, the spatial distribution and composition of carbon sources within these salt marshes can vary systematically with elevation. Specifically, elevation gradients exert a structural force on OM composition by influencing inundation frequency. Lower elevations flood more frequently, experience more prolonged anaerobic conditions, and receive greater tidal inputs of marine and estuarine OM. These differences in inundation regimes, in turn, shape vegetation communities, microbial processes, and sediment dynamics, with elevation serving as a proxy for inundation frequency, salinity stress, root biomass, mineral sediment inputs, and decomposition rates (Janousek et al. 2025b), which might shift the relative contributions of autochthonous and allochthonous OM sources across an elevation gradient. For instance, Peck et al. (2025) observed that soil cores taken near channels and upstream areas had more terrestrial OM. In contrast, those near tideflats and inlets received more estuarine OM, a pattern consistent with the inundation-driven OM delivery varying across an elevation gradient.

Elevation, alongside other more local-scale factors, such as ecosystem type and estuary identity, explains more variance in SOC stocks than regional or climate factors (e.g., climate zone, latitude, ecoregion, estuary type, precipitation, temperature) (Janousek et al. 2025a). In the

PNW, elevation is the most consistent driver of sediment carbon density in tidal wetlands (Kauffman et al. 2020, Janousek et al. 2025b). Despite these patterns, the degree to which elevation structures OM source composition within individual marshes remains poorly characterized, especially using isotopic approaches. Accounting for this gap is critical since PNW coastal high marsh carbon stocks are estimated at 543 ± 47 Mg C/ha, exceeding even the carbon stocks in upland forests of the Coastal Range (Kauffman et al. 2020). While Peck et al. (2025) studied OM source along elevation gradients across different PNW estuaries, they did not examine OM source along elevation gradients within estuaries.

Salt marsh sediments are comprised of a mixture of autochthonous and allochthonous carbon sources, the composition of which spatially varies. For instance, Zhang et al. (2024) studied local carbon sourcing in two Chinese wetlands. They found that allochthonous terrestrial input was the dominant carbon source in one marsh due to increased salinity and strong hydrodynamic conditions. Similarly, Peck et al. (2025) found that Oregon salt marshes are less autochthonous than expected, with 41 ± 6% to 62 ± 4% of sediment OM derived from in situ sources, unlike other U.S. Pacific Coast marshes. In contrast, studies from Washington and California marshes reported substantially higher autochthonous contributions (73 ± 10% to 89 ± 11% and > 88%, respectively; Drexler et al 2020, Ward et al. 2021), highlighting Oregon's high allochthonous character. The relatively high allochthonous contribution in Oregon marshes is hypothesized to be driven by sediment load, a dominant cross-site control on OM sources in these salt marshes, as marshes with high fluvial loads tend to bury more estuarine-derived OM (Peck et al. 2025).

Furthermore, little is known about carbon storage in transitional, recently restored, and sparsely vegetated ecosystems. However, Drexler et al. (2020) noted that restored and reference

marshes in Washington differed in their carbon contributions. Specifically, while reference marshes had greater autochthonous contributions from established vascular plant communities, restored marshes received more allochthonous carbon. Among global blue carbon stocks in coastal ecosystems, O'Connor et al. (2019) noted that restored sites began to store carbon amounts comparable to those of a reference marsh only after 7-17 years post-restoration. Still, most studies lack the temporal and isotopic context to evaluate this trajectory. Furthermore, how elevation structures carbon source composition remains unclear in restored systems (O'Connor et al. 2019). At about 30 years post-restoration, Kunz Marsh, this study's sampling site, sits at an informative point along the restoration recovery trajectory at which its carbon source composition might be expected to reflect a more mature, restored state. Yet characterization of carbon origins within similar restoration trajectories remains relatively limited in the literature, which has large implications for blue carbon finance market implementation within data sparse regions like the PNW (Kauffman et al. 2020).

To address the limited isotopic characterization of OM sources within-marsh elevation gradients and the potential difference between restored and reference marshes in the PNW, we collected surface sediment samples for isotopic analysis at Kunz Marsh, a restored marsh, and Tom's Creek Marsh (TMR), a reference high marsh. This study aims to answer the questions: a) how do soil carbon sources differ across the Kunz Marsh elevation gradient? and b) how do restored and reference high marsh sites differ in their carbon source composition?

Methods

A. Site Description

All sampling sites were located within Kunz Marsh (43.281153ºN, -124.319331ºW) at the South Slough National Estuarine Research Reserve (SSNERR) in Coos Bay, Oregon. The

region experiences a Mediterranean climate with warm, dry summers and cool, wet winters, receiving an average annual precipitation of 164 cm (Schultz et al. 2023). The average tidal range is 2.3 m (Schultz et al. 2023). Kunz Marsh is a 5-hectare tidal salt marsh that was restored in 1996, having previously been diked in the early 1900s for agriculture (Cornu and Sadro 2002). The site was restored to establish three target elevations: low (1.5 m NAVD88), mid (1.8 m), and high (2.2 m). This regrading scheme allowed for quantifying the effects of elevation on the restoration process, specifically surface elevation change, vertical accretion, tidal channel development, emergent vegetation colonization, and fish use (Cornu and Sadro 2002). Elevation cells were initially separated by geotextile cloth to promote independent development within each zone, but it was removed in 2016 (Schultz et al. 2023). Vegetation within the site is elevation-dependent, with *Carex lyngbyei, Deschampsia cespitosa, and Agrostis spp.* dominating the high and mid marsh, while *S. pacifica* dominates the lower cell (Schultz et al. 2023). Tom's Creek Marsh, located about 180 m across Winchester Creek from Kunz Marsh high elevation cell, has an elevation of 2.14 m NAVD88 (Schultz et al. 2023) and served as a reference high marsh. Although historically diked, it was never fully converted for agriculture and has remained tidally influenced for approximately 40 years. (Cornu and Sadro 2002). Vegetation is dominated by *Agrostis stolonifera, Distichlis spicata,* and *Triglochin maritima* (Schultz et al. 2023). Both Kunz and Tom's Creek Marsh experience mesohaline to polyhaline salinity conditions (Schultz et al. 2023).

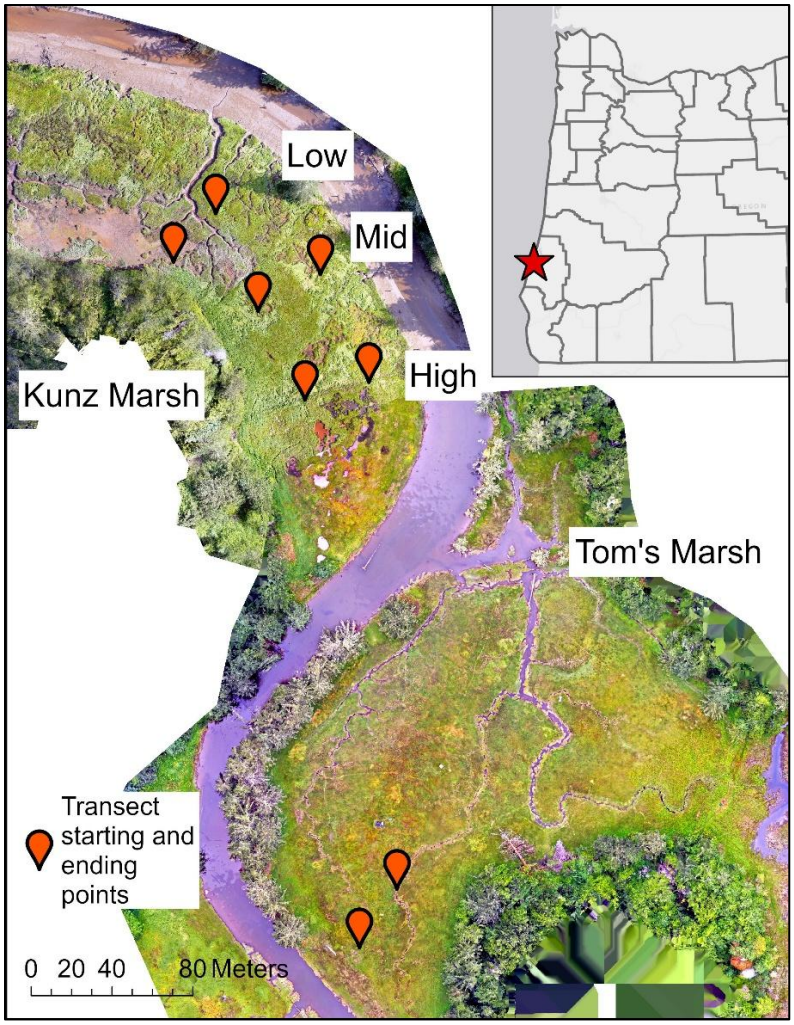


Figure 1.1. Orthomosaic imagery of Kunz Marsh and Tom's Creek Marsh (TMR) within the South Slough National Estuarine Research Reserve (SSNERR), Coos Bay, Oregon. The composite image was produced from two drone surveys: Kunz Marsh (June 24, 2025) and Tom's Creek Marsh (June 23, 2026). The three experimentally manipulated elevation cells of Kunz Marsh (low, mid, and high) are visible, with red markers indicating transect starting and ending points used for stable isotope core collection. The upper right inset shows the location of SSNERR (red star) within Oregon. Oregon country boundary data sourced from U.S. Counties Generalized (Esri, U.S. Census Bureau, NOAA).

B. Soil Core Sampling Design

Surface sediment cores were collected in January 2024 along transects established within each of the three elevation zones within Kunz Marsh: Kunz High (KH), Kunz Middle (KM), and Kunz Low (KL). An additional transect was established at Tom's Marsh (TMR), a reference high-marsh site, following the same sampling protocol as at Kunz Marsh. Each transect was oriented roughly perpendicular to the adjacent creek and spanned 32 m, with 5 sampling points

established at 8 m intervals. Sampling points were numbered sequentially from 1 to 5, with point 1 located nearest to the creek and point 5 furthest. Sampling was conducted on a rising tide.

At each sampling point, three replicate surface sediment cores were collected using a 4-in diameter PVC corer inserted to a depth of 5 cm, yielding 15 cores per elevation zone and 45 cores across all three zones, plus an additional 15 cores from TMR for a total of 60 cores. At KL, the mudflat sediment allowed for straightforward insertion and extraction of the corer. At KM, KH, and TMR, vegetation was first cut around the corer perimeter with a serrated knife to facilitate insertion. The corer and knife were rinsed with site water between sampling points to prevent cross-contamination. After extraction, each core was transferred to a labeled Ziploc bag and frozen until the subsampled material was subsequently processed for stable isotope analysis ($\delta^{13}C$ and $\delta^{15}N$). Although three replicate cores were collected at each of the five sampling points per transect, two samples from KM were not available for stable isotope analysis, resulting in a final per-core dataset of n = 15 for KH, KL, and TMR, and n = 13 for KM.

C. Isotope analysis ($\delta^{13}C$, $\delta^{15}N$)

At each of the five sampling points per transect, three replicate cores were each subsampled two times (e.g., KH 1-1 through KH 1-3), yielding six subsamples per sampling point. Before stable isotope analysis, samples were visually inspected and root-picked using tweezers to remove root material as thoroughly as possible, then oven-dried at 60 ºC and hand-ground using a mortar and pestle. Each subsample consisted of 4.8-5.2 g of soil, weighed on microbalance. Subsamples designated for $\delta^{13}C$ and $\delta^{15}N$ analysis were placed in either silver or tin capsules before being submitted to the University of California, Davis Stable Isotope Facility for natural abundance ^{13}C and ^{15}N analysis. Along with the samples, multiple tins of acetanilide (approximately 2 g each) were included to serve as internal standards. Isotope ratios are reported

in delta notation (‰) relative to Vienna Pee Dee Belemnite (VPDB) for $\delta^{13}C$ and atmospheric air for $\delta^{15}N$. Certified reference materials including Glutamic Acid, Caffeine, Enriched Alanine, and Nylon Powder were used for scale normalization, drift correction, and quality control. Mean reproducibility of reference material replicates was ± 0.11‰ for $\delta^{13}C$ and ± 0.10‰ for $\delta^{15}N$.

D. Statistical analysis

Stable isotope values ($\delta^{13}C$ and $\delta^{15}N$) were first visualized with a biplot to examine isotopic clustering across elevation zones and among sites. Normality of model residuals was assessed prior to analysis using the Shapiro-Wilk test, and non-parametric tests were used where assumptions were violated. To formally test for differences in $\delta^{13}C$ and $\delta^{15}N$ among groups, Kruskal-Wallis tests were conducted separately for each isotope, with Dunn's test used for Bonferroni-corrected pairwise comparisons among elevation zones at Kunz Marsh (KL, KM, KH) and the Tom's Marsh reference site (TMR). All statistical analyses were conducted in R (version 4.6.0).

Carbon source contributions to surface sediment organic matter were estimated using the Bayesian stable isotope mixing model MixSIAR in R (Stock et al. 2018). Samples were grouped by site (KH, KM, KL, and TMR) to assess differences in carbon source composition across the Kunz Marsh elevation gradient and between Kunz Marsh (a restored site) and Tom's Marsh (a reference site). An uninformative Dirichlet prior ($\alpha = 1$) was specified, assigning equal prior probability to all sources. The model used a "long" run setting with 300,000 total iterations, a burn-in of 200,000 iterations, a thinning interval of 100, and 3 chains, yielding 3,000 posterior samples for inference. Source end-member values (means and standard deviations) came from Table S1 in Peck et al. (2025), who compiled previously published PNW stable isotope signatures of potential wetland carbon sources from Drexler et al. (2020) and Howe and

Simenstad (2015). Sources were organized into three broad categories: salt marsh (including *Carex lyngbyei*, *Juncus balticus*, *Triglochin maritima*, *Schoenoplectus maritimus*, and benthic diatoms), terrestrial (including terrestrial C3 plants, *Alnus rubra*, and *Acer circinatum*), and estuarine (including *Zostera marina*, *Ulva lactuca*, marsh C4 plants such as *Distichlis spicata*, benthic diatoms, marine macroalgae, and phytoplankton). Model convergence was assessed using the Gelman-Rubin and Geweke diagnostics, both standard outputs of MixSIAR (Stock et al. 2018). Gelman-Rubin diagnostic values were below 1.05 for all parameters, indicating satisfactory convergence across chains. The Geweke diagnostic indicated that 14 of 82 variables fell outside ±1.96 in one of three chains. However, given consistent results across two independent model runs, these estimates were retained for inference.

Results

A. $\delta^{13}C$ versus $\delta^{15}N$

The $\delta^{13}C$ and $\delta^{15}N$ biplot revealed clear isotopic clustering by elevation zone across Kunz Marsh, with distinct separation between KL, KM, and KH (Figure 1.2). A systematic trend of isotopic enrichment with decreasing elevation was observed, with KL samples exhibiting the highest $\delta^{13}C$ and $\delta^{15}N$ values, KM samples occupying an intermediate position, and KH samples the most depleted in both isotopes. Kruskal-Wallis tests indicated that overall differences among sites were significant for both $\delta^{13}C$ ($\chi^2 = 49.52$, df = 3, $p < 0.001$) and $\delta^{15}N$ ($\chi^2 = 49.63$, df = 3, $p < 0.001$). Dunn's pairwise comparisons revealed significant differences between most site pairs, with three non-significant comparisons: KH and KM were not significantly different in $\delta^{13}C$ ($z = -1.090$, $p = 0.827$), KL and KM were not significantly different in $\delta^{15}N$ ($z = 1.975$, $p = 0.145$), and KH and TMR were not significantly different in $\delta^{15}N$ ($z = 1.795$, $p = 0.218$) (Table 1.1). Tom's Marsh (TMR) showed clear isotopic separation from all three Kunz Marsh elevation

zones, clustering at the most depleted $\delta^{13}C$ and $\delta^{15}N$ values on the biplot (Figure 1.2). Notably, TMR and KH were isotopically distinct despite both representing high marsh environments, with TMR having significantly lower $\delta^{13}C$ ($z = 2.973$, $p = 0.009$) but not significantly different $\delta^{15}N$ ($z = 1.795$, $p = 0.218$) compared to KH.

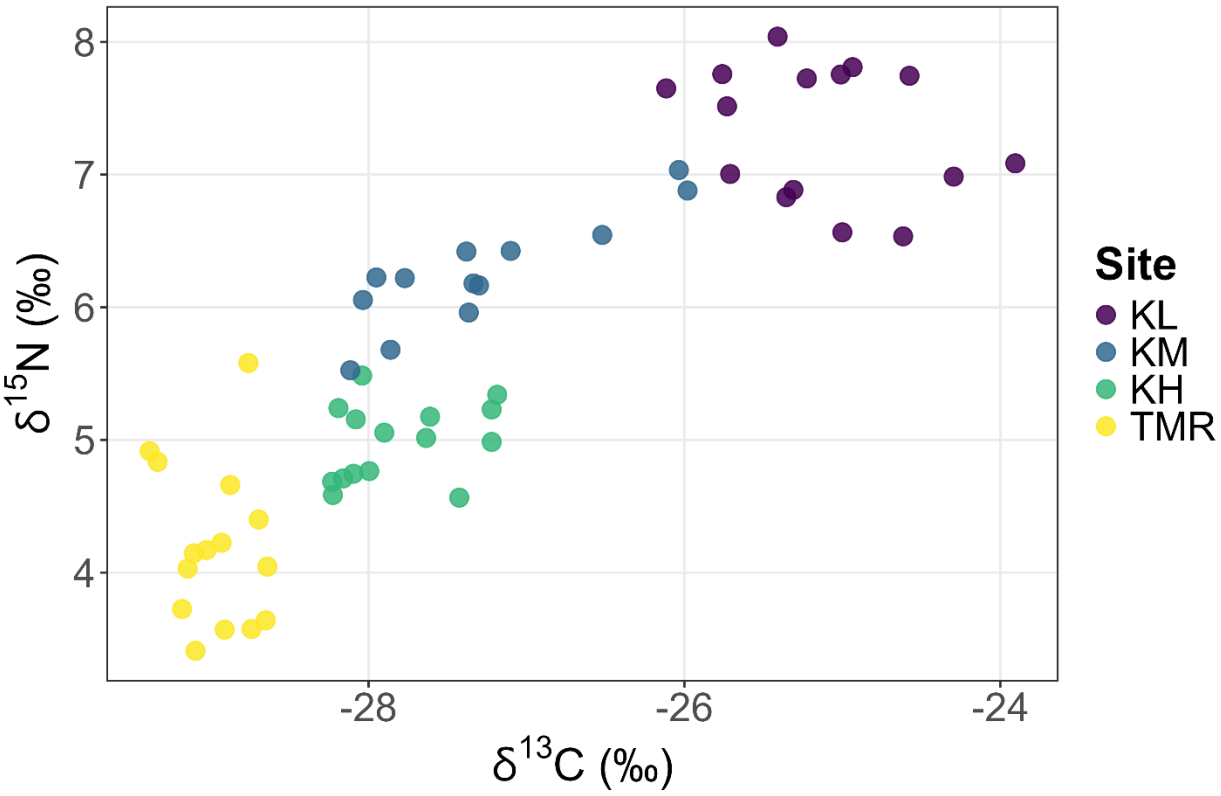


Figure 1.2. Stable isotope biplot of $\delta^{13}C$ and $\delta^{15}N$ values (‰) for surface sediment samples collected across three elevation zones at Kunz Marsh (KL = low, KM = mid, KH = high) and a reference high marsh site at Tom's Marsh (TMR). Each point represents a single core averaged across analytical replicates (KL n = 15, KM n = 13, KH n = 15, TMR n = 15). Elevation zones show distinct isotopic clustering, with KL samples occupying the most enriched $\delta^{13}C$ and $\delta^{15}N$ values, KM samples occupying an intermediate position, and KH and TMR samples clustered at the most depleted $\delta^{13}C$ values and lowest $\delta^{15}N$ values.

Table 1.1. Dunn's pairwise comparisons of $\delta^{13}C$ and $\delta^{15}N$ values among elevation zones at Kunz Marsh (KL = low, KM = mid, KH = high) and Tom's Marsh reference site (TMR). z-scores and Bonferroni-corrected p-values are reported. Overall differences were assessed using Kruskal-Wallis tests ($\delta^{13}C$: $\chi^2 = 49.52$, df = 3, $p < 0.001$; $\delta^{15}N$: $\chi^2 = 49.63$, df = 3, $p < 0.001$). * $p < 0.05$.

	$\delta^{13}C$		$\delta^{15}N$	
Comparison	**z**	**p (adjusted)**	**z**	**p (adjusted)**
KL versus KH	-3.979	< 0.001*	-4.746	< 0.001*
KL versus KM	2.744	0.018*	1.975	0.145
KL versus TMR	6.952	< 0.001*	6.541	< 0.001*

KH versus KM	-1.090	0.827	-2.598	0.028*
KH versus TMR	2.973	0.009*	1.795	0.218
KM versus TMR	3.955	< 0.001*	4.328	< 0.001*

Kruskal-Wallis tests ($\delta^{13}C$: $\chi^2 = 49.52$, df = 3, $p < 0.001$; $\delta^{15}N$: $\chi^2 = 49.63$, df = 3, $p < 0.001$). * $p < 0.05$.

B. Carbon Sources

Salt marsh organic matter was the dominant carbon source across all four sites, though its relative contribution varied across the elevation gradient in Kunz Marsh (Table 1.2, Figure 1.3, Figure 1.4). KL showed the highest salt marsh contribution (mean = 78.0%, 95% credible interval (CrI) [49.4%-92.9%]), followed by KM (mean = 75.9%, 95% CrI [63.8%-86.0%]), and KH (mean = 58.5%, 95% CrI [43.4%-69.7%]). TMR, a reference high marsh, also showed a substantial salt marsh contribution (mean = 51.8%, 95% CrI [33.9%-66.2%]).

Terrestrial organic matter showed a clear inverse pattern with elevation, increasing from KL (mean = 4.70%, 95% CrI [0.90%-11.4%]) through KM (mean = 19.0%, 95% CrI [8.80%-29.8%]) to KH (mean = 34.6%, 95% CrI [23.7%-47.7%]). TMR had the highest terrestrial contribution of all sites (mean = 45.7%, 95% CrI [31.6%-61.9%]), including KH, despite both representing high marsh environments.

Estuarine sources contributed modestly across all sites. KL showed the greatest estuarine contribution (mean = 17.3%, 95% CrI [2.40%-45.4%]), while TMR showed the lowest (mean = 2.50%, 95% CrI [0.20%-8.90%]). KH and KM showed similarly low estuarine contributions (means of 6.90% and 5.00%, respectively).

Table 1.2. MixSIAR posterior estimates of organic matter source contributions (%) for each site. Values represent the percentage of organic matter attributed to each source category. Mean and standard deviation (SD) of the posterior distribution are reported alongside the 2.5th percentile, median (50th percentile), and 97.5th percentile as the 95% credible interval. Sites: KH = Kunz High, KM = Kunz Mid, KL = Kunz Low, TMR = Tom's Marsh reference. Gelman-Rubin diagnostic values were below 1.05 for all parameters; the Geweke diagnostic indicated that 14 of 82 variables fell outside ±1.96 in one of three chains, though results were consistent across independent model runs.

Site	Source	Mean (%)	SD (%)	2.5%	50%	97.5%
KL	Salt marsh	78.0	11.3	49.4	79.8	92.9
	Terrestrial	4.7	2.8	0.9	4.1	11.4
	Estuarine	17.3	11.1	2.4	15.2	45.4
KM	Salt marsh	75.9	5.8	63.8	76.4	86.0
	Terrestrial	19.0	5.3	8.8	18.9	29.8
	Estuarine	5.0	5.3	0.2	3.4	18.5
KH	Salt marsh	58.5	6.8	43.4	59.2	69.7
	Terrestrial	34.6	6.1	23.7	34.1	47.7
	Estuarine	6.9	4.6	1.4	6.1	17.9
TMR	Salt marsh	51.8	8.3	33.9	52.5	66.2
	Terrestrial	45.7	7.8	31.6	45.1	61.9
	Estuarine	2.5	2.7	0.2	1.7	8.9

Model fit: 300,000 iterations; 200,000 burn-in; thinning interval = 100; 3 chains; uninformative Dirichlet prior ($\alpha = 1$). DIC = -23.36.

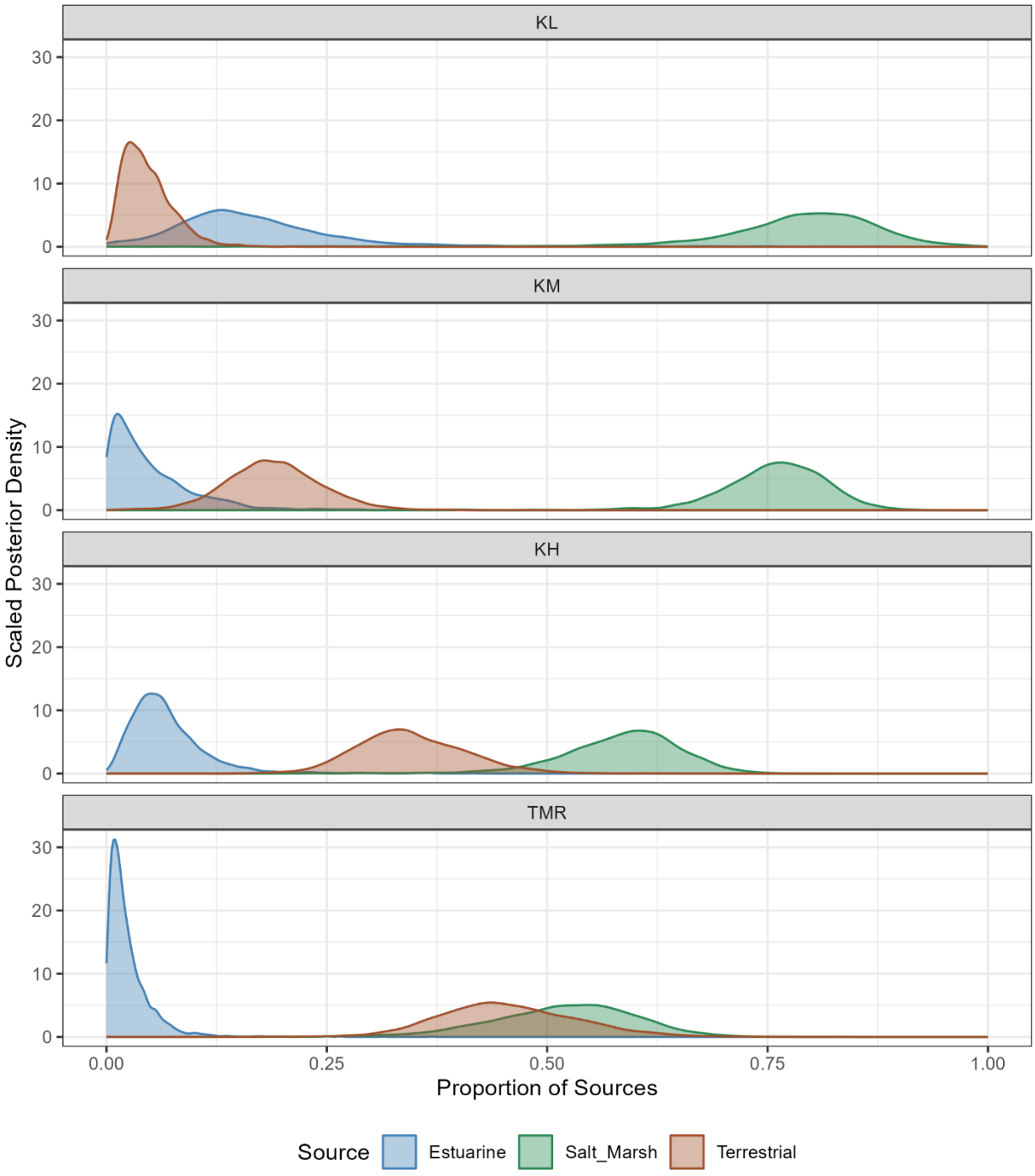


Figure 1.3. Posterior probability density distributions of organic matter source contributions (%) estimated by mixSIAR for each site: Kunz Low (KL), Kunz Mid (KM), Kunz High (KH), and Tom's Marsh reference site (TMR). The x-axis represents the estimated proportion of each source contributing to sediment organic matter. The y-axis shows scaled posterior density. Wider, flatter distributions indicate greater uncertainty in source estimates. Source categories are salt marsh, terrestrial, and estuarine, as defined by end-member values synthesized from Peck et al. (2025).

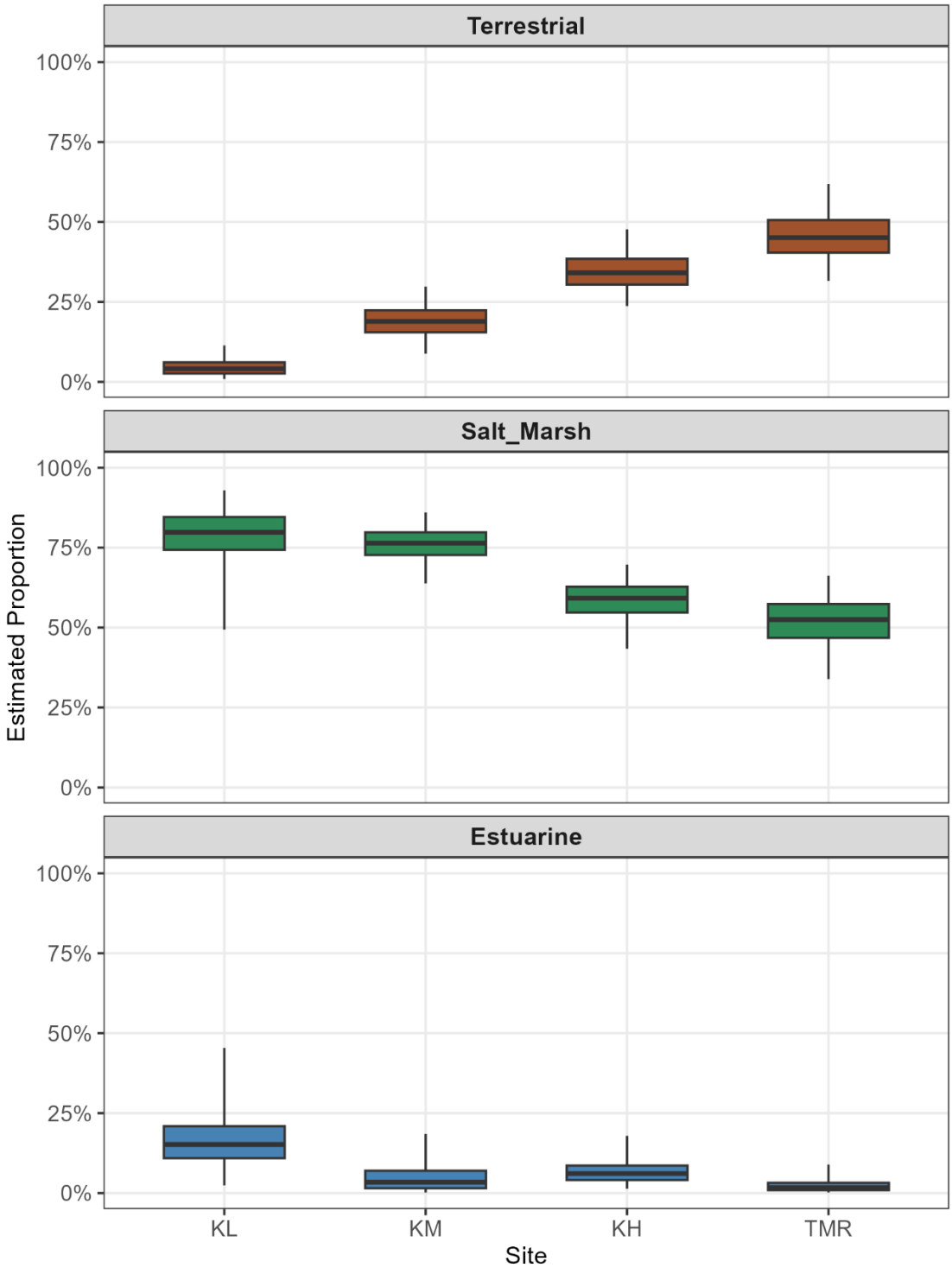


Figure 1.4. Posterior distributions of organic matter source contributions (%) estimated by MixSIAR for each site across three source categories: estuarine, salt marsh, and terrestrial. Sites include Kunz Low (KL, n =15), Kunz Mid (KM, n = 13), Kunz High (KH, n = 15), and Tom's Marsh reference site (TMR, n = 15), where n reflects the number of surface sediment cores used as mixture inputs. Boxes represent posterior credible intervals (median, 25th-75th percentiles, 2.5th-97.5th percentiles) from MixSIAR. Source end-member values were drawn from Peck et al. (2025). Posterior summary statistics are reported in Table 1.2.

Discussion

This study examined how elevation and restoration structures organic matter source composition in a restored PNW tidal salt marsh, addressing two research questions. Carbon source composition differed significantly across the Kunz Marsh elevation gradient: salt-marsh-derived OM dominated across all zones but decreased with elevation, terrestrial contributions increased with elevation, and estuarine contributions remained low throughout but peaked in the low marsh. Organic matter source composition also differed between the restored high marsh (KH) and the reference high marsh (TMR) despite their shared high elevation category, with TMR showing higher terrestrial and lower salt marsh and estuarine contributions than KH. Together, these findings suggest that both elevation and restoration history are meaningful factors that structure carbon source composition in PNW tidal marshes, with implications for how restored marshes are monitored, evaluated against reference conditions, and ultimately included within blue carbon accounting frameworks.

The isotopic composition of surface sediment differed significantly across all elevation zones at Kunz Marsh. Specifically, as elevation decreased from KH to KM to KL, $\delta^{13}C$ and $\delta^{15}N$ values increased, indicating enrichment with decreasing elevation. This enrichment may reflect two concurrent processes. First, increased anaerobic microbial nitrogen processing at lower elevations, particularly denitrification, preferentially removes ^{14}N and enriches residual $\delta^{15}N$ in the substrate. Second, greater tidal connectivity at lower elevations increases the influence of marine and estuarine organic matter sources, which tend to be more enriched in $\delta^{13}C$ and $\delta^{15}N$ relative to terrestrial C3 inputs (Peterson et al. 1985, Craft et al. 1988). The MixSIAR model results are consistent with the latter interpretation, showing the highest estuarine contribution at KL, though it remained modest relative to salt marsh and terrestrial sources. The low

contribution of estuarine sources overall is expected given Kunz Marsh's inland position within the reserve, located about 12 km upstream from the mouth of South Slough, where marine influence is reduced with increasing channel distance from Coos Bay (Peck et al. 2025).

While most elevation pairings differed significantly in their $\delta^{13}C$ and $\delta^{15}N$ compositions, some exceptions were noted. KH and KM were not distinguishable in their $\delta^{13}C$ values, and KL and KM did not differ significantly in their $\delta^{15}N$ values. The KH and KM overlap in $\delta^{13}C$ values suggests that KH and KM might be experiencing similar carbon processes, while the KL and KM $\delta^{15}N$ overlap may reflect comparable nitrogen cycling dynamics despite their different tidal inundation regimes. In contrast, the significant $\delta^{15}N$ difference between KH and KM suggests greater denitrification activity in the more tidally influenced KM zone.

The reference site, TMR, showed a partially distinct isotopic composition from KH, despite both being categorized as high-elevation sites. TMR had significantly lower $\delta^{13}C$ values than KH, though $\delta^{15}N$ values did not differ significantly between the two sites. The depleted $\delta^{13}C$ signature at TMR relative to KH is consistent with isotopic signatures reported for reference marshes in the PNW, where terrestrial C3 plant inputs, which tend to be more depleted in $\delta^{13}C$, contribute more to sediment organic matter (Drexler et al. 2020, Peck et al. 2025). The non-significant $\delta^{15}N$ difference may reflect similar nitrogen cycling dynamics between the two high marshes despite their different restoration histories. However, the MixSIAR contribution estimates, which show higher terrestrial contributions at TMR than at KH, suggest that overall carbon source composition can differ even where isotopic signatures overlap.

Salt marsh dominance decreased with increasing elevation across Kunz Marsh, while terrestrial contributions showed the opposite pattern. The elevated terrestrial contribution at KH is consistent with the dense vegetation cover at higher elevations relative to KL, which was

largely unvegetated. KH may also receive more terrestrial inputs from the adjacent upland forest, which might accumulate rather than be exported due to limited tidal flushing at higher elevations. This is consistent with findings from Peck et al. (2025), who found that cores located furthest upstream and away from tidal inlets tended to receive more terrestrially sourced OM, while those closer to tidal flats and inlets received proportionally more estuarine material, a spatial pattern analogous to the elevation gradient observed here. Although both salt marsh and terrestrial end-members are predominantly C3 plants and therefore overlap in $\delta^{13}C$ values, environmental conditions such as salinity and tidal inundation influence which species are present at a given elevation, thereby influencing the isotopic composition of the local OM pool (Craft et al. 1988). Specifically, the salt marsh category includes salt-tolerant species such as *Carex* and *Juncus*. In contrast, terrestrial species such as *Alnus rubra* would not persist under the saline or brackish conditions of lower marsh zones. The strong separation in $\delta^{15}N$ between these two source categories and their associated vegetation provided sufficient resolution to distinguish between them across most elevation pairings, underscoring the value of using multiple isotopic tracers. In contrast, the estuarine source category includes *Zostera marina* (eelgrass) and C4 plants such as *Distichlis spicata*, which have more enriched $\delta^{13}C$ values, indicating greater marine and tidal influence. While *D. spicata* was documented in low abundance in the low marsh zone and eelgrass has been observed near Hinch Bridge just downstream of Kunz Marsh as recently as 2016, neither species was abundant at the site during a 2023 vegetation survey by SSNERR staff. This limited abundance is consistent with the low estimated estuarine contribution across all elevation zones.

MixSIAR results showed that TMR had proportionally higher terrestrial contributions and lower salt marsh and estuarine contributions compared to KH, despite both sites representing

high marsh environments in proximity. These findings suggest that more mature high marsh environments may accumulate proportionally greater terrestrial OM over time. Whether this reflects a successional trajectory in which terrestrial OM accumulation contributes to elevation gain and reduced tidal connectivity over time warrants further investigation. Drexler et al. (2020) found that restoring marsh sites had proportionally more allochthonous carbon relative to reference sites, and that source composition differences reflected the degree and duration of restoration. If TMR is a reference marsh, then the restored Kunz high marsh has not yet reached the same composition as a mature high marsh. This has implications for management, specifically regarding what constitutes a "successful" restoration and the duration of recovery required to match a reference marsh eventually (Drexler et al. 2020). While O'Connor et al. (2019) estimated that restored sites may require 17 or more years to reach parity with reference sites in carbon storage quantity, the timeline for convergence in carbon source composition specifically remains unknown. This uncertainty has implications for restoration monitoring and management. If isotopic convergence with reference sites takes decades, as with carbon storage quantity, short-term restoration funding cycles typically spanning one to three years may be insufficient to capture meaningful recovery signals, highlighting the need for long-term monitoring plans that can track restoration trajectory over ecologically relevant time scales. More broadly, salt marsh-derived OM, produced in situ, was the dominant source across all sites, suggesting that autochthonous production plays a central role in sediment carbon composition at Kunz Marsh. However, allochthonous contributions from terrestrial and estuarine sources were non-trivial, with terrestrial inputs increasing with elevation and estuarine inputs decreasing with elevation and peaking in the low marsh. This observation is broadly consistent with Peck et al. (2025), who found that autochthonous salt marsh sources comprised the largest fraction of

sediment OM across high elevation salt marsh sites in Oregon. However, their contribution ranged widely (41 ± 6% to 62 ± 4%) and allochthonous sources were not negligible. The Kunz high marsh estimated contribution of 58.5% salt marsh, or autochthonous carbon, falls within this range, suggesting that the autochthonous character of Kunz Marsh is broadly comparable to other Oregon high marshes studied by Peck et al. (2025).

This study has several limitations worth noting. Since core sampling was conducted in January 2024, carbon source composition may vary seasonally, as precipitation and tidal dynamics influence allochthonous carbon delivery, particularly at higher elevations, where terrestrial inputs may increase with runoff (Mitrovic and Baldwin 2016). Sediment accretion rates at Kunz Marsh are relatively high (2.9 ± 0.24 mm/yr) compared to other Oregon marshes (Eidam et al. 2024), and may differ across elevation cells, meaning that a single sampling depth may capture different lengths of depositional time across the elevation gradient, complicating comparisons of organic matter source composition between zones and between KH and TMR. Finally, diagenesis, driven largely by microbial decomposition, can shift stable isotope values by 1-2‰ over periods as short as 13 months, with $\delta^{15}N$ changing more than $\delta^{13}C$ (Greiner et al. 2016; Jankowska et al. 2016; Drexler et al. 2020). $\delta^{15}N$ values, particularly in lower-elevation zones where anaerobic conditions are more persistent, should therefore be interpreted with appropriate caution, as they may partly reflect post-depositional alteration rather than source composition alone.

More broadly, these findings contribute to a growing body of work showing that wetland restoration holds significant potential as a nature-based climate solution. Restored tidal wetlands are increasingly recognized as cost-effective mechanisms for increasing carbon storage and supporting blue carbon market development, given their capacity to sequester carbon at rates that

justify restoration investment (Hao et al. 2024). However, realizing this potential requires that restored sites ultimately recover the ecological function of and carbon dynamics of wetlands, a trajectory that, as this study demonstrates, may take decades and requires long-term monitoring to evaluate meaningfully (Craft 2022). As blue carbon markets continue to expand, particularly in data-sparse regions like Oregon in the PNW, where carbon stocks are substantial but poorly characterized, especially in origin, studies that document carbon source composition and recovery trajectories in restored marshes will be increasingly important for informing future carbon accounting methodologies.

Questions remain about how allochthonous carbon should be accounted for in carbon budgets and balances, given that it is complicated to measure. Drexler et al. (2020) similarly argues that allochthonous carbon should not be excluded from carbon accounting, as it comprises a substantial portion of the sediment carbon sink in both restored and reference marshes. Given that autochthonous salt marsh sources dominate at Kunz Marsh, allochthonous carbon accounting may be less of a concern here than at more hydrologically open sites, though seasonal variation remains uncharacterized. The elevation-dependent carbon source patterns observed here raise the question of whether carbon cycling processes, including decomposition, sequestration, and greenhouse gas emission, also vary systematically across the elevation gradient. Whether the carbon within these marshes' elevation gradients is sequestered or emitted back into the atmosphere remains a recognized gap in blue carbon research more broadly (Drexler et al. 2020, Janousek et al. 2025a).

Conclusion

The elevation gradient at Kunz Marsh reflected distinct $\delta^{13}C$ and $\delta^{15}N$ isotopic signatures indicating variation in carbon sources across the elevation gradient. Salt marsh-derived carbon

was the dominant source across the gradient, though its relative contribution decreased with increasing elevation. In contrast, terrestrial carbon contribution increased with elevation, likely reflecting decreasing tidal connectivity from the low to the high marsh, where terrestrial carbon accumulates rather than washing away with the tides. Estuarine carbon contribution remained relatively low throughout the marsh but was highest in the low-elevation cell, consistent with greater tidal connectivity at lower elevations.

This biogeochemical distinction across elevation zones was expected given that elevation drives differences in salinity and tidal conditions, which in turn shape vegetation communities and microbial processes. Low marshes experience greater tidal connectivity and inundation and typically mirror the salinity of the adjacent creek or ocean. In contrast, mid- and high marshes are less inundated and might become hypersaline as standing water evaporates, concentrating residual salts. Between the restored high marsh (KH) and the reference high marsh (TMR), KH showed lower terrestrial carbon contributions than TMR, indicating that the restored site has not yet matched the reference marsh in its carbon source composition despite both representing high marsh environments.

While the isotope biplot revealed mostly distinct $\delta^{13}C$ and $\delta^{15}N$ values across the elevation gradient, indicating distinct carbon sources, the MixSIAR model quantified the relative contributions of terrestrial, estuarine, and salt marsh end-member sources in each elevation cell. Stable isotopes, along with the MixSIAR model, identified carbon sources present across the elevation gradient at Kunz Marsh and in what proportion, but the fate of that carbon remains unresolved. Future work is needed to determine whether this carbon is ultimately sequestered, exported, or emitted to the atmosphere as CO_2 or CH_4, and whether this fate differs by source. Specifically, whether the same source-based distinctions observed across the elevation gradient

at Kunz Marsh are mirrored in CO_2 and CH_4 flux patterns remains an open question. This question is addressed directly in Chapter V, which examines greenhouse gas flux dynamics across the same elevation gradient.

V. GREENHOUSE GAS FLUX DYNAMICS ACROSS A SALT MARSH ELEVATION GRADIENT

Introduction

Tidal salt marshes play a paradoxical role in the global carbon cycle by functioning as substantial carbon sinks while being significant natural emitters of methane (CH_4), a potent greenhouse gas (GHG). The same anaerobic, waterlogged conditions that slow organic matter decomposition and promote long-term carbon storage also drive methanogenesis, producing CH_4, a GHG with approximately 80 times the warming potential of CO_2 over a 20-year horizon (IPCC 2023). As such, the balance between these two dynamics, which is influenced by environmental conditions that vary across space and time, determines whether a given salt marsh functions as a net source or sink of carbon. Salinity is one such environmental variable. Elevated salinity acts as a proxy for increased sulfate availability in sediments, causing sulfate-reducing bacteria to outcompete methanogens and suppressing CH_4 production (Arias-Ortiz et al. 2024). Tidal inundation is another environmental variable, as it controls the depth and duration of anaerobic conditions within the soil profile, governing redox conditions, microbial community composition, and the balance between aerobic decomposition and methanogenesis (Arias-Ortiz et al. 2024). Complicating this further is a wetland's land-use history, which can alter carbon cycling dynamics. Restored marshes are typically subsided and disconnected from their natural tidal flow (Cornu and Sadro 2002), which differs from that of reference marshes in their hydrological regimes, organic matter pools, and microbial communities. Subsequently, these differences might influence net GHG fluxes in ways that are not yet well understood.

Elevation is a well-documented driver of GHG flux, especially CH_4, in salt marshes, largely because it integrates the effects of tidal inundation, salinity, and vegetation community

across a marsh elevation gradient (Comer-Warner et al. 2022, Shahan et al. 2022, Arias-Ortiz et al. 2024, Janousek et al. 2025a, Williams et al. 2025). The expected pattern is that lower elevations, which have greater tidal connectivity and more anaerobic conditions, emit more CH_4. In contrast, higher elevations, which are typically drier and more aerobic, tend to have lower CH_4 emissions (Comer-Warner et al. 2022, Williams et al. 2025). The CO_2 flux pattern across elevation gradients is less clear, partly because it includes the interplay between photosynthetic uptake and ecosystem respiration, both of which can vary with vegetation community composition and species-specific productivity traits (Cherry et al. 2009, Kirwan et al. 2009, Langley et al. 2009, Ratliff et al. 2015). High marsh zones, which are typically more densely vegetated and drier than frequently inundated low marsh zones, might therefore be expected to have higher photosynthetic CO_2 uptake and lower CH_4 emissions.

Critically, the complex carbon dynamics of tidal salt marshes are undercharacterized in regions such as the Pacific Northwest, especially in Oregon. Carbon storage and stocks in PNW tidal wetlands are better studied than gas fluxes, and existing gas flux studies are geographically concentrated in Washington and California, leaving Oregon underrepresented. Gas flux studies have become more feasible with the availability of portable gas analyzers (used with static chambers) that provide continuous measurements with limited user handling. Schultz et al. (2023) provided one of the most comprehensive measurements of chamber-based GHG fluxes across two different Oregon estuaries with different management regimes, finding that CH_4 emissions were highly variable and dependent on multiple environmental drivers operating across spatial and temporal scales. Despite this variability, most sites showed net CO_2 removal over 20- and 100-year timeframes, and restoration of wetlands in more saline areas of estuaries was identified as most likely to yield net climate benefits, given that high salinity suppresses CH_4

emissions. More recently, Williams et al. (2025) expanded on these findings by examining flux dynamics across restored and reference tidal marshes, highlighting the role of elevation, salinity, and water table depth in controlling CH_4 emissions. Nevertheless, key gaps remain in the current understanding of within-marsh elevation-gradient fluxes, and diel-scale dynamics are especially understudied (Arias-Ortiz et al. 2024). Seasonal chamber measurements dominate the literature, while continuous 24-hour measurements, which could separate the contributions of respiration and photosynthesis, remain rare due to the logistical challenges of nighttime and inundated sampling in tidal environments and the high cost of automated chamber systems.

Another underexplored mechanism governing CH_4 flux in vegetated wetlands is plant-mediated gas transport. Many wetland plants possess aerenchyma, plant tissue with large, air-filled spaces for gas exchange between the shoot and root (Sculthorpe, 1967), that act as conduits for CH_4, bypassing oxidation within the soil profile where it would otherwise be consumed (Brix et al. 1992, Verville et al. 1998). This transport pathway can substantially increase CH_4 emissions relative to diffusion alone (Comer-Warner et al. 2022). However, aerenchyma plays a dual role in that it simultaneously delivers O_2 to the root zone, creating an oxidized rhizosphere that suppresses methanogenesis locally (Frenzel and Rudolph 1998). The net effect of plant-mediated transport on CH_4 emissions therefore depends on the balance between these two competing functions, which varies with plant species, vegetation density, and soil conditions. How these factors interact with local hydrology and soil conditions remains poorly understood.

To address these gaps, this study examined CO_2 and CH_4 flux dynamics at Kunz Marsh, a restored tidal salt marsh within the South Slough National Estuarine Research Reserve (SSNERR) in Coos Bay, Oregon. Specifically, this chapter aims to answer the following questions: a) what environmental drivers govern seasonal CO_2 and CH_4 fluxes across the Kunz

Marsh elevation gradient? b) how do CO_2 and CH_4 fluxes differ at diel scales, and what environmental variables drive flux under light and dark conditions? and c) what does diel partitioning of light and dark CO_2 flux reveal about the balance between ecosystem respiration and gross primary production at the high marsh of Kunz?

Methods

A. Site Description

Greenhouse gas flux sampling was conducted at Kunz Marsh, located within the South Slough National Estuarine Research Reserve (SSNERR) in Coos Bay, Oregon, as described in Chapter IV. Kunz Marsh was experimentally graded into low-, mid-, and high-elevation zones, all with approximately equal areas (low: 0.54 ha, mid: 0.56 ha, high: 0.53 ha) (Cornu and Sadro 2002). While Kunz Marsh does contain two low-elevation zones, only the first (Kunz low 1 as described by Cornu and Sadro (2002)) was used in this study. Tidal inundation decreases markedly with elevation at Kunz Marsh: the low cell experiences between 5.91 and 7.12 hours of inundation per day on average, the mid cell between 2.25 and 3.61 hours, and the high cell between 0.18 and 0.84 hours (Cornu and Sadro 2002). Vegetation composition within the site was characterized using 2023 SSNERR survey data. *Carex lyngbyei* is the dominant vascular plant across all elevation zones, with peak abundance in the mid-elevation zone and lower abundance in the high and low zones. The low marsh, while sparsely vegetated, supports the greatest species richness, including *Zostera japonica* (though only counted once), umbellifer species, and macroalgae, reflecting its greater tidal connectivity and inundation frequency. The mid-elevation zone functions as a transitional zone, with *Carex* remaining dominant alongside greater graminoid diversity. The high marsh is dominated by *Carex lyngbyei* and *Deschampsia cespitosa*, with wrack and woody debris also present. Despite dense vegetation patches, bare

cover in the high marsh was comparable to or exceeded that in the lower-elevation zones, likely reflecting the patchy spatial structure of high-marsh vegetation and localized ponding. The low marsh, while largely unvegetated in vascular plants compared with the mid and high zones, supports a diverse group of intertidal and estuarine species consistent with its mudflat character. Field access to the marsh was via a trail through the adjacent upland forest and about the same access routes were followed on each sampling day to minimize disturbance.

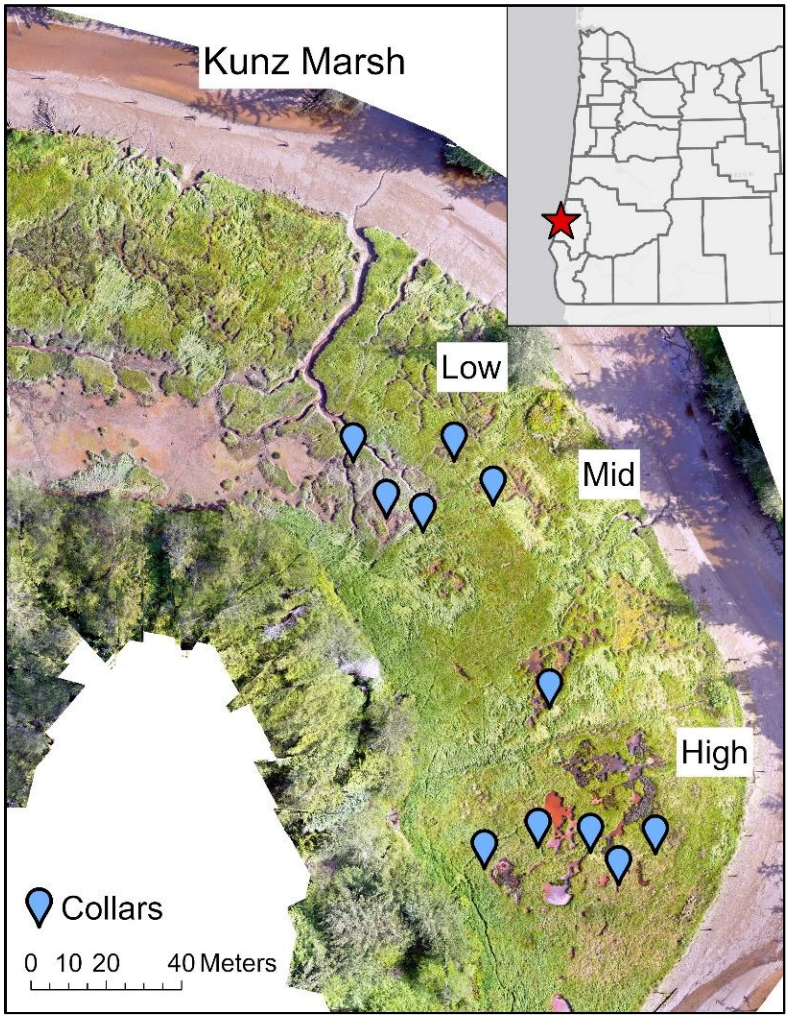


Figure 2.1. Drone orthomosaic imagery of Kunz Marsh within the South Slough National Estuarine Research Reserve (SSNERR), Coos Bay, Oregon taken on June 24, 2025. The three experimentally manipulated elevation cells of Kunz Marsh (low, mid, and high) are visible, with blue markers indicating collars used for greenhouse gas flux collection. The upper right inset shows the location of SSNERR (red star) within Oregon. Oregon country boundary data sourced from U.S. Counties Generalized (Esri, U.S. Census Bureau, NOAA).

B. Seasonal Greenhouse Gas Flux Sampling

Carbon dioxide and methane fluxes were measured in situ using a portable Fourier-transform infrared (FTIR) trace gas analyzer (LI-COR LI-7810) connected in a closed-loop system to two "stackable" transparent static chambers. The lower chamber rested on the collar and had a radius of 19.3 cm and a height of 31.6 cm; the upper chamber rested on the lower and had a radius of 19.4 cm and a height of 32 cm. Combined, the two chambers enclosed a volume of 0.0748 m^3 over a collar area of 0.1225 m^2. The chamber frame was constructed from PVC with cutout “windows” covered by transparent greenhouse film to fully enclose the tall marsh vegetation present at sampling locations. A small battery-powered fan mounted inside the chamber ensured thorough mixing of headspace air during measurements.

Collars were fabricated from the same PVC material and installed by pressing them into the soil. Since collar insertion depth varied with soil conditions, the height of each collar extending above the ground surface was measured individually and used to calculate the headspace volume for that collar. To minimize soil disturbance effects on gas flux, measurements were not taken until at least 48 hours after collar installation. A total of nine collars were deployed across the three elevation cells, with three collars per cell (low marsh: LM1-LM3; mid marsh: MM1-MM3; high marsh: HM1-HM3). Collars in the low and mid elevation cells were drilled with three evenly spaced holes around the circumference to allow tidal water exchange consistent with ambient conditions. These holes were plugged with rubber stoppers during sampling.

For each measurement, the chamber was seated on the collar and sealed as airtight as field conditions permitted for a duration of six minutes. To minimize flux disturbance from soil compaction or ebullition caused by movement near the collars, boardwalks were installed at each

collar location. All nine collars were sampled on each of seven sampling days: July 7, July 14, August 4, August 11, August 12, September 3, and September 19, 2025. Sampling on the two July dates occurred in the afternoon (approximately 3:45-5:30 PM and 2:05-4:00 PM, respectively), as the sampling protocol was still being refined and tidal inundation of the low and some mid elevation collars constrained access to periods of low tide. Beginning in August, sampling was conducted in the morning between approximately 8:00 AM and 1:00 PM to standardize conditions across dates.

C. Diel Greenhouse Gas Flux Sampling

A 24-hour sampling campaign was conducted on August 21, 2025, to capture diel patterns in CO_2 and CH_4 flux. The same portable FTIR gas analyzer (LI-COR LI-7810) and closed-loop chamber protocol described in Section B were used for all measurements. Sampling took place continuously from 00:00 to 23:59, with each of the five high marsh collars measured once per hour over 24 consecutive hours.

Two additional collars (HM4 and HM5) were deployed alongside the original three high marsh collars (HM1-HM3) exclusively for the diel campaign to increase replication within the high marsh. These collars were not included in seasonal flux measurements due to timing constraints and to maintain balanced sampling across elevation cells. Diel sampling was restricted to the high marsh given the logistical challenges of conducting nighttime flux measurements in a tidal marsh environment, including but not limited to, safety concerns, labor requirements, and the absence of automated chamber equipment.

D. Environmental Covariates

Environmental covariates for statistical modeling were obtained from four sources: continuous meteorological monitoring data from the South Slough NERR System-Wide

Monitoring Program (SWMP), continuous water level data from the National Oceanic and Atmospheric Administration (NOAA) tide station 9432780 (Charleston, Oregon), field measurements taken concurrently with flux sampling, and drone-based multispectral imagery collected by SSNERR staff.

Air temperature, relative humidity, and photosynthetically active radiation (PAR) were obtained from the SSNERR SWMP Tom's Creek meteorological station (station code: SOSTCMET; 43.27913°N, 124.31837°W), which records data at 15-minute intervals and undergoes a standardized multi-tiered QA/QC process managed by the Centralized Data Management Office. Provisional plus data have passed both automated range and error checking and a secondary review by Reserve staff, while provisional data have passed only the initial automated checks. Meteorological data used in this study were predominantly provisional plus, except for data from September 19, 2025, which remained at provisional status at the time of analysis.

For seasonal flux sampling, porewater salinity was measured in the field concurrent with each sampling event using a handheld refractometer. Where available, porewater was extracted from a PVC porewater channel installed adjacent to each collar. In practice, field collection was sometimes limited by turbid or difficult-to-filter porewater reducing sample quality. When a porewater channel was unavailable or porewater could not be reliably collected, salinity values were substituted with concurrent measurements from the South Slough NERR SWMP Winchester Arm water quality station (station code: SOSWIWQ; 43.28242°N, 124.32032°W). For the 24-hour sampling campaign, salinity was obtained exclusively from the Winchester Arm water quality station due to the sparse temporal resolution of field-collected porewater measurements.

Collar elevation was measured in the field using Real Time Kinematic (RTK) GPS with a Reach RS3 rover and base station. A fixed base station established by South Slough NERR staff (-124.320956°W, 43.282253°N; ellipsoidal height 4.395 m) provided satellite error corrections, and the rover, equipped with tilt compensation, was placed at the center of each collar for a single point elevation measurement. Raw coordinates were subsequently projected into NAD83(2011)/UTM zone 10N+NAVD88 (GEOID12B) to match the coordinate system of drone imagery.

Water level data (m NAVD88) were obtained from the NOAA tide station rather than the Winchester Arm water quality station, as the latter is not vertically controlled. The NOAA station therefore serves as an approximation of local water level conditions. Estimated water table depth at each collar was calculated by subtracting NOAA water level from RTK-surveyed collar elevation, where positive values indicate the collar is above the water surface and negative values indicate inundation. Estimated water table values were later mean-centered separately for each dataset (seasonal and 24-hour) by subtracting each collar's mean water table depth across the respective sampling dates. This accounts for between-collar differences in absolute elevation and expresses each observation as a deviation from that collar's typical water table conditions within each sampling context. Positive deviations indicate drier than average conditions for that collar, while negative deviations indicate wetter than average conditions.

Vegetation greenness was characterized for each collar using the Normalized Difference Vegetation Index (NDVI) derived from a drone-based multispectral survey conducted by NERR staff on June 24, 2025. NDVI values were extracted in ArcGIS by applying a circular buffer with a radius of 19.4 cm around each collar's recorded GPS coordinate, approximating the area

enclosed by the collar, and averaging all pixel values within the buffer. This yielded a single mean NDVI value per collar, which was treated as a static covariate across all sampling dates.

E. Statistical Analyses

Greenhouse gas fluxes were calculated from time-series concentration data recorded by the LI-COR LI-7810 using the R package fluxfinder. Prior to flux calculation, the first minute of each 6-min chamber deployment was removed across all sampling dates to eliminate chamber placement effects, as visual inspection of concentration-versus-time plots revealed rapid, non-representative increases in gas concentration immediately following chamber placement. Linear slopes were then derived from the remaining 5-min measurement window for each deployment. Flux estimates were retained for further analysis if the linear fit met quality thresholds of $R^2 > 0.3$ and $p < 0.05$, following criteria similarly applied by Williams et al. (2025). Flux outputs were converted to μmol m^{-2} min^{-1} to standardize measurements and facilitate comparison with previous studies conducted at similar sites. Seasonal and diel flux datasets were treated separately throughout all analyses; diel measurements were not included in the seasonal flux models.

Seasonal Flux Models

Seasonal CO_2 flux was modeled using a linear mixed model (LMM) fit by restricted maximum likelihood (REML) using the lme4 and lmerTest packages in R. Fixed effects included marsh surface elevation, soil temperature, air temperature, total PAR, mean NDVI, salinity, and estimated water table deviation. Site (collar ID) was included as a random intercept to account for repeated measurements across sampling dates at the same location. Significance of fixed effects was assessed using Satterthwaite's method.

Seasonal CH_4 flux was log-transformed prior to analysis to meet normality assumptions. A generalized additive mixed model (GAMM) was fit using the mgcv package in R to accommodate the nonlinear relationship between mean NDVI and CH_4 flux. Mean NDVI was included as a penalized thin-plate regression spline smooth term, while all remaining predictors (marsh surface elevation, soil temperature, air temperature, total PAR, salinity, and estimated water table deviation) were included as parametric fixed effects. Site (collar ID) was included as a random intercept. Normality of model residuals was assessed using the Shapiro-Wilk test and no outlier removal was necessary as residuals met normality assumptions following log-transformation of CH_4 flux. Model fit was assessed using adjusted R^2 and AIC.

Diel Flux Models

For the 24-hour diel campaign, flux measurements were partitioned into dark and light periods based on concurrent PAR measurements. Observations where PAR is 0 mmol m^{-2} were classified as dark period measurements, and observations where PAR is greater than 0 mmol m^{-2} were classified as light period measurements. Dark period measurements theoretically represent ecosystem respiration in the absence of plant photosynthetic activity.

To assess whether flux differed significantly between light and dark periods, separate LMMs were first fit for CO_2 and CH_4 with period (light versus dark) as a fixed effect and collar ID as a random intercept. Following this, environmental drivers of CO_2 flux were examined separately for dark and light periods using two additional LMMs, each with collar ID included as a random intercept. Fixed effects for the light period model included estimated water table deviation, total PAR, soil temperature, air temperature, mean NDVI, and salinity. PAR was excluded from the dark period model due to zero variance during nighttime hours, but all remaining predictors were retained. Outliers identified through residual inspection were removed

prior to final model fitting where necessary. All statistical analyses were conducted in R (version 4.6.0).

Results

A. Seasonal Carbon Dioxide Flux

A linear mixed model identified total PAR and air temperature as significant predictors of CO_2 flux (Table 2.1). Total PAR had a significant negative effect ($\beta = -0.188$, SE = 0.051, $p < 0.001$), while air temperature had a significant positive effect ($\beta = 37.50$, SE = 10.06, $p < 0.001$). All remaining fixed predictors (soil temperature, NDVI, salinity, and water table deviation) were non-significant ($p > 0.05$). Elevation was not a significant predictor of CO_2 flux ($\beta = 90.59$, SE = 102.10, $p = 0.408$), though a positive directional trend was observed with increasing elevation (Figure 2.2B). Considerable among-site variation was captured by the random intercept (site-level SD = 62.48). Fixed effects alone explained 30% of variance in CO_2 flux (marginal $R^2 = 0.30$), with site-level random effects accounting for an additional 29% (conditional $R^2 = 0.59$), indicating a relatively balanced contribution of environmental drivers and spatial variation.

Table 2.1. Linear mixed model results for CO_2 flux (μmol m^{-2} min^{-1}). Fixed effects include environmental and site-level predictors. Random intercepts were estimated for each site (ID). * $p < 0.05$.

Fixed Effects					
Predictor	**β**	**SE**	**df**	**t**	**p**
Intercept	526.62	780.48	25.99	0.675	0.506
RTK elevation	90.59	102.10	6.19	0.887	0.408
Soil temperature	-51.95	41.07	26.81	-1.265	0.217
Air temperature	37.50	10.06	28.52	3.728	< 0.001*
Total PAR	-0.188	0.051	26.53	-3.712	< 0.001*
NDVI (mean)	-198.78	307.82	8.09	-0.646	0.536
Salinity	-1.333	3.058	28.88	-0.436	0.666
Water table deviation	-41.11	31.45	27.13	-1.307	0.202
Random Effects					
Group	**Variance**	**SD**			
Site (ID)	3904	62.48			

Residual	5737	75.74

Model fit: N = 37 observations, 9 sites; REML criterion = 375.0. * $p < 0.05$.

B. Seasonal Methane Flux

A generalized additive mixed model identified NDVI as the only significant predictor of CH_4 flux (Table 2.2). NDVI had a significant nonlinear effect on CH_4 flux (edf = 2.33, F = 7.234, p = 0.001), with intermediate vegetation density associated with the highest flux values and declining flux at both low and high NDVI (Figure 2.2A). All parametric predictors (soil temperature, air temperature, total PAR, salinity, and water table deviation) were non-significant ($p > 0.05$). Elevation was not a significant predictor of CH_4 flux ($\beta = 1.211$, SE = 1.058, p = 0.296), though a positive directional trend with increasing elevation was observed (Figure 2.2B), consistent with CO_2. Considerable among-site variation was present in the random effect structure (site SD = 0.542), indicating meaningful site-level differences in CH_4 flux independent of the measured predictors. Fixed effects alone explained a moderate proportion of variance in log-transformed CH_4 flux (marginal $R^2 = 0.22$), while the inclusion of site-level random effects substantially improved model fit (conditional $R^2 = 0.86$), indicating that among-site variation was the dominant driver of CH_4 flux rather than the measured environmental predictors.

Table 2.2. Generalized additive mixed model (GAMM) results for CH_4 flux (log-transformed; μmol m^{-2} min^{-1}). Parametric coefficients include environmental and site-level predictors; s(NDVI mean) is a penalized thin-plate regression spline. Random intercepts were estimated for each site (ID). Adjusted $R^2 = 0.724$; AIC = 98.33; n = 39. Significance code: * $p < 0.05$.

Parametric Coefficients					
Predictor	**β**	**SE**	**df**	**t**	**p**
Intercept	-4.822	5.501	-	-0.877	0.388
RTK elevation	1.371	1.030	-	1.331	0.193
Soil temperature	0.075	0.302	-	0.249	0.805
Air temperature	0.053	0.072	-	0.739	0.466
Total PAR	-0.0003	0.0004	-	-0.947	0.351

Salinity	-0.023	0.022	-	-1.048	0.303
Water table deviation	-0.327	0.207	-	-1.584	0.124
Smooth Term					
Predictor	**edf**	**Ref.df**		**F**	**p**
s(NDVI mean)	2.33	2.33	-	7.234	0.001*
Random Effects					
Group	**Variance**	**SD**			
Smooth basis (Xr)	-	9.457			
Site (ID %in% g)	-	0.542			
Residual	-	0.486			
Model fit: N = 39, 9 sites; Adj. R^2 = 0.724; Scale est. = 0.236; AIC = 98.33; BIC = 116.63; log-likelihood = -38.16. * $p < 0.05$.					

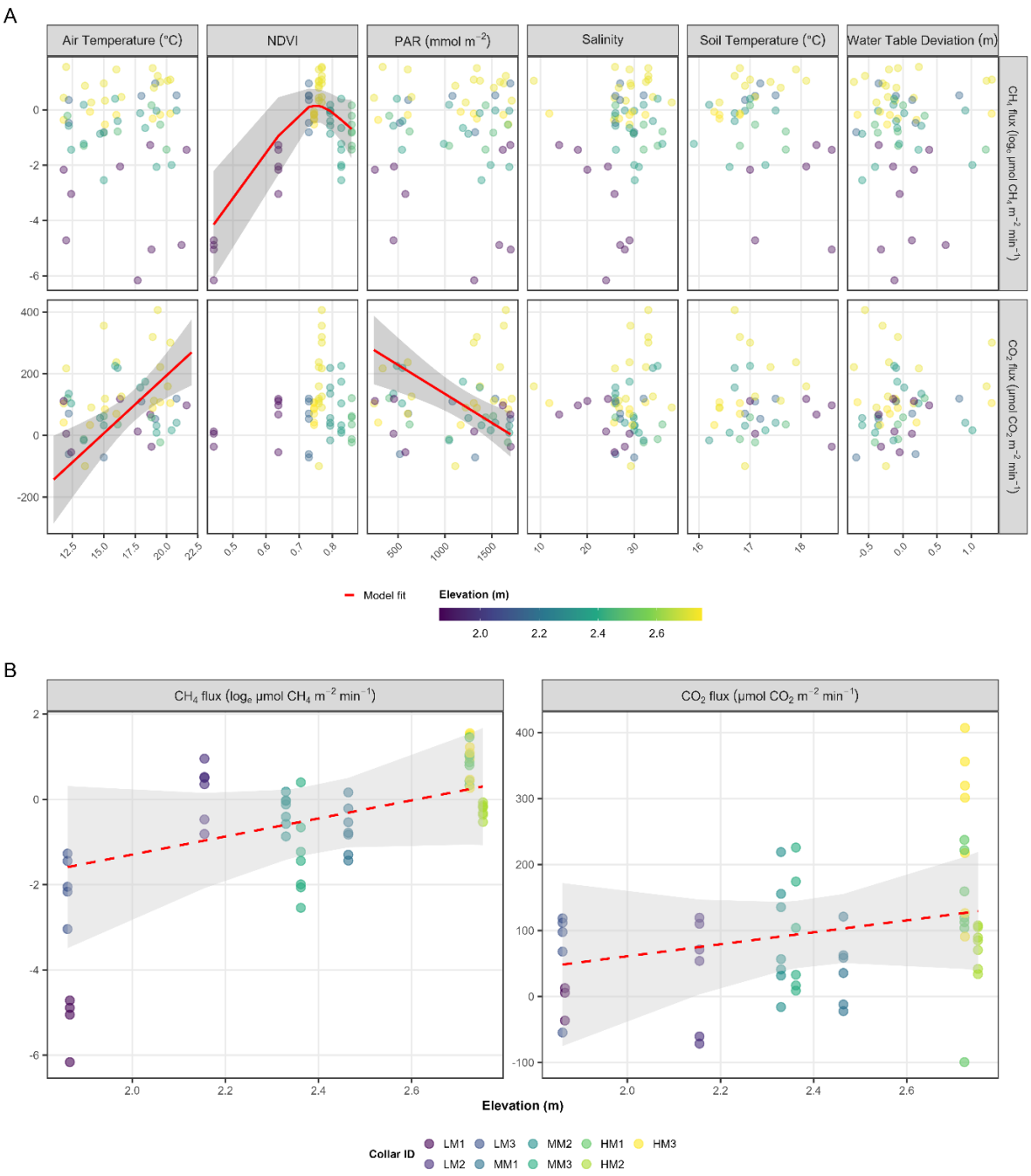


Figure 2.2. Relationships between greenhouse gas fluxes and environmental predictors **(A)** and marsh surface elevation **(B)** across nine collars (low marsh: LM1-LM3; mid marsh: MM1-MM3; high marsh: HM1-HM3). Points in **(A)** are colored by marsh surface elevation (m NAVD88) while points in **(B)** are colored by collar ID. Solid red lines **(A)** indicate statistically significant model-fitted relationships ($p < 0.05$) with 95% confidence intervals (shaded): NDVI for CH_4 (GAMM) and air temperature and PAR for CO_2 (LMM). Panels without a line indicate non-significant predictors. Dashed red lines **(B)** show LMM fitted values regardless of significance. Neither CH_4 nor CO_2 flux showed a statistically significant relationship with elevation ($p > 0.05$).

C. Diel Flux Dynamics for Carbon Dioxide and Methane

Visual inspection of CO_2 and CH_4 flux across the 24-hour sampling period revealed no strong diel trends in either gas (Figure 2.3). Both CO_2 and CH_4 flux showed a general decline around 07:00, though no consistent pattern was observed across the remainder of the day. Visually, CH_4 flux also remains relatively more stable compared to CO_2 flux throughout the sampling period.

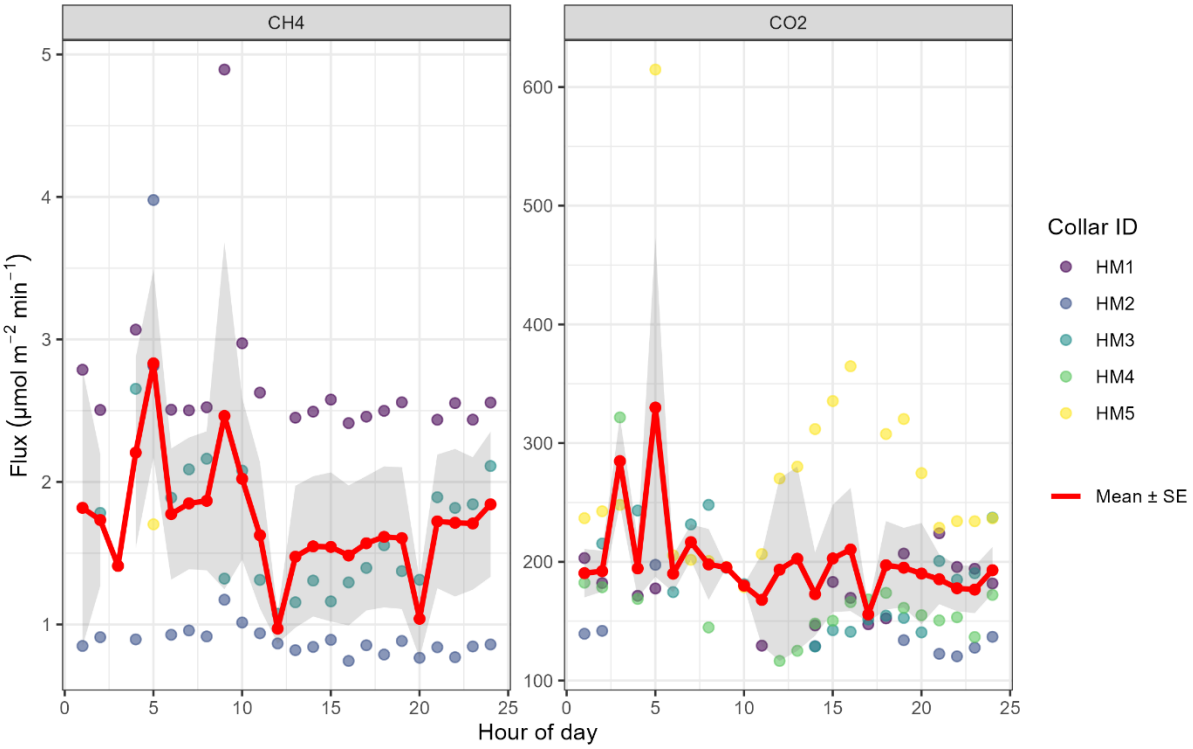


Figure 2.3. Diel patterns in CH_4 and CO_2 flux (µmol m^{-2} min^{-1}) measured across five high marsh collars (HM1-HM5) during the 24-hour sampling campaign conducted on August 21, 2025, at Kunz Marsh. Colored points represent individual collar flux measurements at each hour. The red line and points indicate the hourly mean flux across all collars; the grey ribbon represents standard error.

A linear mixed model with collar ID as a random intercept confirmed that CO_2 flux differed significantly between dark and light periods (β = -0.109, SE = 0.043, df = 7.62, t = -2.549, p = 0.013), with light period fluxes lower than dark period fluxes on average (Figure 2.4A). CH_4 flux did not differ significantly between light and dark periods (β = -0.077, SE = 0.047, df = 61.09, t = -1.628, p = 0.109) (Figure 2.4A). Mean ecosystem respiration, or dark period (PAR = 0) CO_2 fluxes averaged across all collars, was 203.46 ± 13.49 µmol m^{-2} min^{-1}

(mean ± SE) (Figure 2.4B). Net ecosystem exchange (NEE), derived from light period (PAR > 0) measurements, was 191.18 ± 9.41 µmol m^{-2} min^{-1}. Gross primary production (GPP), calculated as respiration minus NEE and expressed as a negative value to reflect carbon uptake, was -12.29 ± 16.45 µmol m^{-2} min^{-1}.

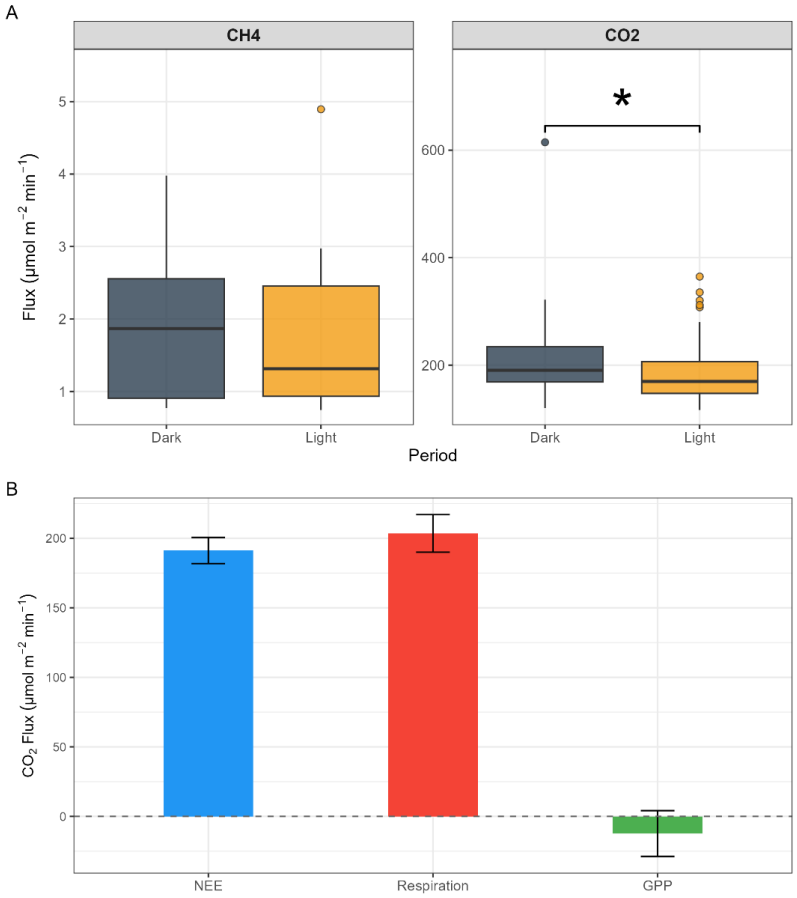


Figure 2.4. Greenhouse gas flux measurements from the 24-hour sampling campaign conducted on August 21, 2025, across five high marsh collars (HM1-HM5) at Kunz Marsh. **(A)** Boxplots of CH_4 and CO_2 flux (µmol m^{-2} min^{-1}) partitioned by light and dark periods. **(B)** Mean CO_2 flux (µmol m^{-2} min^{-1}) for net ecosystem exchange (NEE), ecosystem respiration, and gross primary production (GPP). NEE represents mean flux from all light period measurements, respiration represents mean flux from all dark period measurements, and GPP was calculated as respiration minus NEE. GPP is presented as a negative value to reflect carbon uptake. Error bars represent standard error. The dashed line indicates zero flux. These estimates reflect a single late-summer sampling campaign during a period of likely reduced plant productivity due to seasonal senescence, and ecosystem respiration was treated as constant across the 24-hour period. These values should be interpreted as a constrained estimate of carbon fluxes at the high marsh under late-summer conditions and do not represent a full seasonal or annual carbon budget.

No environmental predictors were significant drivers of CO_2 flux during the dark (Figure 2.5A) or light (Figure 2.5B) periods ($p > 0.05$). Similarly, no environmental predictors were significant drivers of CH_4 flux during the dark (Figure 2.6A) and light (Figure 2.6B) periods ($p > 0.05$). Notably, chamber-level random variance was the key driver of variability across all CO_2 and CH_4 flux models, consistently exceeding residual variance (CO_2: ID variance = 1631.7 dark, 3673 light versus residual = 332.6 dark, 1971 light; CH_4: ID variance = 0.443 dark, 0.359 light versus residual = 0.037 dark, 0.018 light). CH_4 especially showed strong chamber-level variance, with ID variance exceeding residual variance by roughly 12-fold in the dark model (0.443 versus 0.037) and 20-fold in the light model (0.359 versus 0.018).

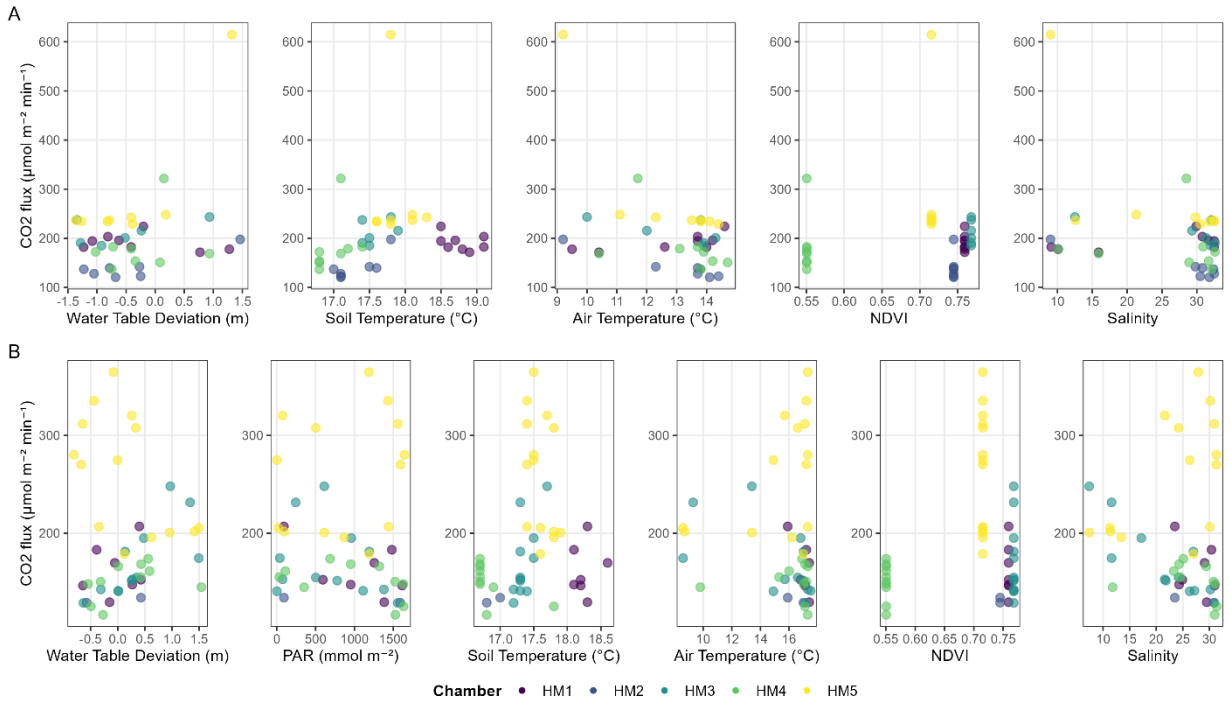


Figure 2.5. Relationships between CO_2 flux (µmol m^{-2} min^{-1}) and environmental predictors during dark **(A)** and light **(B)** periods measured across five high marsh collars (HM1-HM5) during the 24-hour sampling campaign at Kunz Marsh on August 21, 2025. Points are colored by collar ID. Separate linear mixed models were fit for dark and light periods with collar ID included as a random intercept and no environmental predictors were significant.

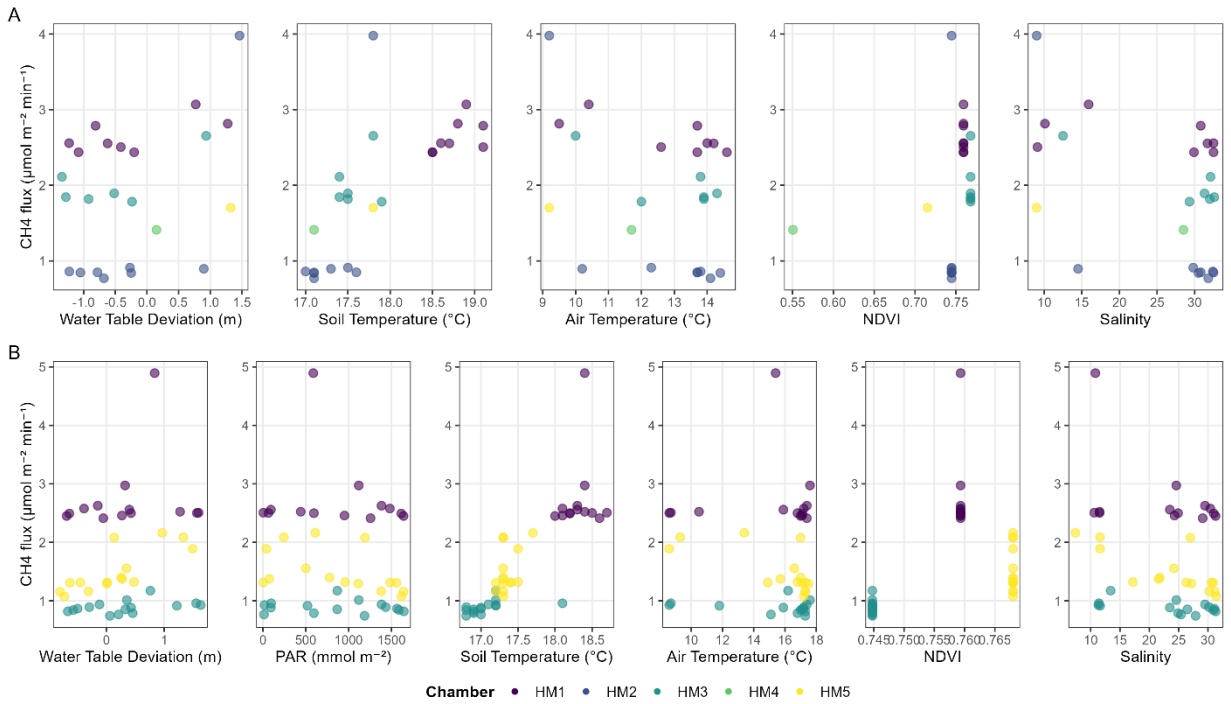


Figure 2.6. Relationships between CH_4 flux (μmol m^{-2} min^{-1}) and environmental predictors during dark **(A)** and light **(B)** periods measured across five high marsh collars (HM1-HM5) during the 24-hour sampling campaign at Kunz Marsh on August 21, 2025. Points are colored by collar ID. Separate linear mixed models were fit for dark and light periods with collar ID included as a random intercept and no environmental predictors were significant.

Discussion

Contrary to expectations in the literature, elevation was not a significant driver of either CO_2 or CH_4 fluxes at Kunz Marsh (Comer-Warner et al. 2022, Shahan et al. 2022, Arias-Ortiz et al. 2024, Janousek et al. 2025a, Williams et al. 2025). Instead, chamber-level variation, especially for CH_4, was the primary driver of gas flux rather than elevation and other measured environmental variables. This trend suggests that what is an elevation effect, or lack thereof, may actually reflect a microsite effect governed by belowground microbial and plant conditions (Moseman-Valtierra et al. 2016, Noyce and Megonigal 2021, Comer-Warner et al. 2022). However, this interpretation should be noted with the caveat that, although the elevation gradient spans from low to high (1.861 m NAVD88-2.754 m NAVD88), replication was limited due to field logistics. Some measurement days occasionally excluded one or more chambers due to equipment limitations or tidal timing constraints that prevented access to flooded collar

locations. The relatively limited replication across the elevation gradient makes it challenging to fully disentangle elevation and microsite effects, especially for CH_4 flux and Kunz Marsh, which exhibits high spatial variability.

At the diel scale, CH_4 flux was similar in both light and dark periods, whereas CO_2 flux was significantly lower during light periods than dark periods. The absence of a light-period effect on CH_4 is consistent with the interpretation that CH_4 flux is governed primarily by microsite-scale conditions rather than by atmospheric drivers. For CO_2, the difference in flux between light and dark periods is consistent with photosynthetic uptake during daylight hours (PAR > 0) suppressing net CO_2 efflux, a pattern well-documented in tidal marsh systems (Forbrich and Giblin 2015, Ruiz-Plancarte et al. 2026). Despite this expected mechanism, PAR did not significantly drive CO_2 flux, even during light periods, likely due to high chamber variance and limited replication, which can dilute the signal and reduce statistical power to detect PAR's influence. Nonetheless, the observed reduction in CO_2 flux during light periods remains ecologically consistent with photosynthetic uptake as the underlying driver (Wimalasekera 2019, Forbrich and Giblin 2015).

Seasonally, CO_2 flux was significantly influenced by PAR and air temperature, indicating sensitivity to short-term atmospheric drivers at seasonal timescales. This contrasts with the diel dataset, where neither PAR nor air temperature was a significant driver despite spanning similar ranges in soil and air temperatures. Temperature is a well-established driver of respiration rates, with respiration generally increasing up to a species or system-specific optimum before declining (Sage and Kubien 2007, Niu et al. 2024). The absence of a detectable temperature effect at the diel scale despite similar temperature ranges as seasonal measurements therefore suggests that timescale-specific mechanisms, rather than differences in environmental conditions alone, may

govern the relationship between atmospheric drivers and CO_2 flux at this site. CO_2 flux may instead respond to cumulative or lagged conditions rather than to instantaneous temperature. Lag effects of 1.5-3.0 hours between photosynthetically active radiation and soil respiration have been documented in upland forest systems, attributed to the transport time of recently fixed carbohydrate to belowground tissue (Mitra et al. 2019). Longer-term legacy effects of past temperature exposure on respiration have also been shown in laboratory incubations (Adekanmbi et al. 2022). However, these systems are upland, grassland, or non-saline wetland, and may not directly translate to the tidally influenced, saline conditions at Kunz Marsh. A simpler explanation is that high chamber-level heterogeneity and limited replication in the diel dataset reduced the statistical power to detect potential environmental drivers. Regardless of the mechanism, CO_2 flux at this site appears more sensitive to sustained or cumulative environmental shifts than to instantaneous changes within a day, which has implications for how flux measurements across different timescales should be interpreted and integrated.

Based on calculated respiration values from the diel dataset, the estimated gross primary productivity of the high marsh was -12.29 ± 16.45 μmol m^{-2} min^{-1}. The large uncertainty relative to the estimate (with the standard error exceeding the absolute mean) suggests that this value should be interpreted with caution and treated as a constrained approximation rather than a precise characterization of ecosystem productivity. A limitation of the Kunz GPP estimate is that the respiration value used in the calculation was held constant over the 24 hours, so it did not account for variability due to temperature or other factors that influence respiration rates (Niu et al. 2024). It is also worth noting that sampling occurred in late August, when marsh vegetation at this site is likely approaching or entering senescence, potentially resulting in lower photosynthetic activity than would be observed during peak growing season. This estimate

therefore represents a late-summer snapshot rather than a comprehensive characterization of annual productivity. Nevertheless, this approach provides a numerical baseline estimate of GPP and NEE under late-summer high marsh conditions at Kunz.

These results are important because, as the climate changes, higher temperatures might increase both plant productivity and organic matter decomposition within salt marshes, with the direction and magnitude of these responses varying by latitude, species composition, and local optimum temperature thresholds (Kirwan et al. 2009, Kirwan and Blum 2011). Whether warming enhances photosynthetic uptake, accelerates decomposition, or both, will determine whether salt marshes function as net sources or sinks of atmospheric CO_2 under future climate change. Vegetation community composition is central to this dynamic, especially within restored marshes. Studies have shown that increased plant productivity and biomass, whether driven by elevated CO_2, temperature, or species-specific traits, can enhance marsh elevation gain, carbon accretion, and organic sediment deposition, while growing season length correlates with productivity across latitudinal gradients (Cherry et al. 2009, Kirwan et al. 2009, Langley et al. 2009, Ratliff et al. 2015). *Carex lyngbyei,* the dominant vascular plant across all elevation zones at Kunz Marsh, with greatest abundance in the mid-elevation zone (SSNERR Vegetation Survey 2023), is a productive marsh sedge characterized by substantial belowground biomass, with root and rhizome biomass consistently exceeding aboveground biomass, and high seasonal aboveground productivity during the spring growing period (Kistritz et al. 1983). Its disproportionate contributions to both carbon storage and CH_4 plant transport via aerenchyma tissue (Turner 1996) make it a particularly important species for understanding the climate trajectory of this restored marsh. As restored marshes like Kunz continue to develop their vegetation communities through natural colonization from adjacent reference marshes,

monitoring *Carex* cover, productivity, and community composition over time in restored marshes may offer insight into carbon sequestration function recovery rates.

For CH_4 flux, microsite conditions accounted for most of the variance at both diel and seasonal scales. Beyond chamber-level heterogeneity, NDVI was the only significant driving factor of seasonal CH_4 flux, with a nonlinear relationship suggesting a potential "sweet spot" mechanism between plant-mediated transport and root oxidation at Kunz Marsh (Fritz et al. 2011, Waldo et al. 2019, Comer-Warner et al. 2022). Aerenchyma tissue plays two competing roles in CH_4 dynamics. It can act as a suppressor by delivering O_2 near the roots, thereby reducing CH_4 production by enabling oxidation locally (Fritz et al. 2011, Waldo et al. 2019). On the other hand, it also acts as a direct conduit that bypasses oxidation entirely in the soil profile, enhancing CH_4 emissions into the atmosphere (Frenzel and Rudolph 1998, Bellisario et al. 1999, Colmer 2003). The observed pattern in which mid-elevation zones with higher NDVI showed lower CH_4 flux than the high marsh, while the low marsh with lower NDVI also showed lower flux, is consistent with this dual role, suggesting that intermediate vegetation density may maximize net CH_4 emissions by balancing plant transport capacity against oxidative suppression. It is worth noting that SSNERR 2023 landscape-level vegetation survey data show *Carex lyngbyei* abundance peaking at mid elevation rather than high. However, NDVI was measured at the collar scale using a 19.4 cm buffer, and the patchy spatial structure of high marsh vegetation may result in locally dense *Carex* areas at individual collar locations that are not fully captured by site-wide abundance counts.

C. lyngbyei, the dominant plant across the Kunz elevation gradient, contains aerenchyma tissue through which CH_4 is passively transported (Whiting and Chanton 1992, Turner 1996), and may therefore play a disproportionate role in CH_4 venting at this site (Arias-Ortiz et al.

2024). This potential role might help explain why CH_4 emissions were higher in the high marsh than in the expected low marsh, which typically experiences more frequent inundation and more anaerobic conditions, both associated with higher CH_4 emissions in comparable systems (Comer-Warner et al. 2022, Williams et al. 2025). The aerenchyma-mediated transport pathway may offset the expected inundation-driven pattern by preferentially venting CH_4 in zones where *C. lyngbyei* density is sufficient to support meaningful plant transport, even where overall vegetation cover is spatially heterogeneous. Further research is needed to fully characterize how root morphology, water table depth, light conditions, salinity, and species-specific traits of *C. lyngbyei* interact to regulate CH_4 emissions across the elevation gradient and at different temporal scales at Kunz Marsh.

Although elevation was not a significant predictor in either the CO_2 or CH_4 seasonal flux models, a positive directional trend was observed for both gases, with flux increasing toward higher elevation zones. This pattern is particularly noteworthy for CH_4, where it runs counter to the typical expectation that lower, more frequently inundated and anaerobic environments favor greater methanogenesis and CH_4 emissions (Comer-Warner et al. 2022, Williams et al. 2025). Schultz et al. (2023) studied GHG fluxes across land management types in the PNW, and similarly found that the low elevation cell of Kunz Marsh had low CH_4 emissions despite having higher water tables and attributed this to the absence of vascular plants, which provide substrate for methanogens and an aerenchyma-based conduit for CH_4 plant release to the atmosphere. This finding and possible explanation is consistent with the pattern observed in this Kunz Marsh study, where CH_4 flux was higher in the high marsh, which despite exhibiting a patchy vegetation structure and comparable bare cover to lower zones (SSNERR 2023 Vegetation Survey), may support dense *C. lyngbyei* patches that, through their aerenchyma tissue, could

provide substantial transport capacity for CH_4, relative to the low marsh where vascular plant cover was sparser despite greater tidal inundation. The observed increase in CH_4 flux toward the high marsh suggests that plant-mediated transport by plants such as *C. lyngbyei* may be offsetting the methanogenic advantage that more anaerobic low-marsh soils would otherwise provide. The mechanism behind the analogous CO_2 trend is less clear. However, differences in plant community composition across the elevation gradient, and their influence on overall productivity and the balance between photosynthetic uptake and respiration, may offer one possible explanation. This elevation-related trend should be interpreted as a suggestive pattern rather than a confirmed effect and warrants further investigation with greater replication across elevation zones.

Surprisingly, salinity and water level were not significant predictors of CO_2 or CH_4 flux, despite their well-known influence on GHG emissions in wetlands, especially CH_4 (Arias-Ortiz et al. 2024, Comer-Warner et al. 2022, Williams et al. 2025). This finding may be partly explained at this site if CH_4 flux is primarily controlled by plant-mediated transport and microsite-level belowground conditions (Moseman-Valtierra et al. 2016, Noyce and Megonigal 2021, Comer-Warner et al. 2022), rather than by coarser-scale environmental hydrological variables such as salinity and water table depth. However, this interpretation should be treated with caution, given that salinity was obtained from the Winchester Arm water quality station about 95 m upstream of the closest low marsh collar and water level from the NOAA tide station at Charleston, Oregon, which monitors conditions closer to the mouth of Coos Bay rather than within the reserve where Kunz Marsh is located. This coarser sampling resolution might thus not be fine enough to capture the variability between each chamber. Future research should prioritize

collecting more frequent, in situ chamber-level measurements of salinity and water table depth to better resolve their potential influence on CO_2 and CH_4 fluxes at this site.

More broadly, future research in similar salt marsh systems should consider tracking CO_2 fluxes by capturing seasonal dynamics. Infrequent seasonal sampling may miss meaningful variability due to environmental drivers operating on cumulative or lagged timescales, so more frequent sampling is needed. In contrast, CH_4 flux measurements should prioritize denser spatial replication, through more chambers within each elevation zone, to account for high-level variance and the effects of microsite conditions, which dominated flux variability in this study. Scaling beyond the chamber level entirely, eddy covariance (EC) towers are a complementary approach and provide high-frequency, landscape-scale measurements of ecosystem metabolism (Morin et al. 2017, Bansal et al. 2023). EC has been applied successfully in coastal wetland systems to capture ecosystem-scale CO_2 and CH_4 dynamics that static chambers cannot fully resolve (Lu et al. 2017, Chu et al. 2021, Arias-Ortiz et al. 2024). Given the scarcity of eddy covariance measurements in Oregon tidal wetlands (Lu et al. 2017, Chu et al. 2021), establishing long-term EC infrastructure at sites like Kunz Marsh would make a meaningful contribution to regional carbon flux monitoring and help ground-truth the chamber-based findings presented here within a landscape-scale context.

Conclusion

Contrary to expectations from the literature, elevation was not a significant predictor of CO_2 or CH_4 flux across the Kunz Marsh elevation gradient, though a suggestive positive directional trend was observed for both gases. Particularly for CH_4, chamber-level variation dominated flux variability at both seasonal and diel timescales, suggesting that microsite-scale belowground conditions, rather than broader-scale environmental drivers, exert primary control

over gas flux at Kunz Marsh. Microsite conditions and plant-mediated transport via aerenchyma-containing species such as *Carex lyngbyei* emerged as the primary drivers of CH_4 gas flux at this site, potentially explaining why CH_4 flux was higher in the more vegetated high marsh than in the frequently inundated low marsh. In contrast, CO_2 flux responded to short-term atmospheric forcings (PAR and air temperature) at seasonal timescales and was lower during light than dark periods at the diel scale, consistent with photosynthetic CO_2 uptake. Together, these patterns suggest that CO_2 flux at this site is more responsive to sustained or cumulative environmental conditions than to instantaneous within-day variation, a distinction with implications for how gas flux measurements across different timescales should be interpreted.

Kunz Marsh was a consistent net source of CO_2 and CH_4 across seasonal sampling dates (mean CO_2 = 96.04 μmol m^{-2} min^{-1}; mean CH_4 = 1.16 μmol m^{-2} min^{-1}), with high collar-level variation in both gases, but particularly for CH_4. Using mean diel dark and light period CH_4 flux (1.76 ± 0.11 μmol CH_4 m^{-2} min^{-1}) as a conservative proxy for total CH_4 flux (given that light and dark period fluxes did not differ significantly) and converting to CO_2-equivalent units using the 20-year global warming potential (80 times according to IPCC 2023) yields 140.8 μmol CO_2-eq m^{-2} min^{-1} (range: 132.2-149.4). This CO_2-equivalent CH_4 flux is about 11-12 times greater than the GPP estimate derived from diel light-dark CO_2 flux partitioning (-12.29 ± 16.45 μmol CO_2 m^{-2} min^{-1}), suggesting that CH_4 emissions substantially offset photosynthetic carbon uptake at the high marsh during the diel sampling period. However, this comparison should be treated with considerable caution, as the GPP estimate carries high uncertainty, reflects a single late-summer campaign when vegetation is likely approaching senescence, and was derived under the assumption of constant respiration. These values are best interpreted as a constrained estimate of carbon flux conditions at the high marsh under late-summer conditions rather than a

characterization of annual carbon balance. Nevertheless, this estimate indicates that CH_4 emissions constitute a meaningful climate forcing at this site and warrant further quantification.

More broadly, the observed flux patterns of CO_2 and CH_4 at Kunz Marsh contribute to a growing body of work on carbon dynamics in restored tidal marshes, with implications for monitoring and evaluating restoration progress. The finding that Kunz Marsh functioned as a net GHG source during the sampling period, while noting that this reflects seasonal snapshots, nonetheless raises questions about the timeline over which restored marshes transition toward net climate benefits. These questions are critical for blue carbon market crediting and restoration investment decisions, especially as wetland restoration gains attention as a potential climate mitigation strategy. The net climate forcing of Kunz Marsh will likely evolve as it accretes more sediment, vegetation communities develop, and plant-mediated transport dynamics shift in response to changing inundation regimes. However, the direction and rates of these changes remain uncertain without long-term monitoring data.

Characterizing GHG flux dynamics across elevation gradients and various timescales in restored marshes like Kunz Marsh is important for assessing whether restoration delivers genuine and reliable climate benefits, particularly as blue carbon markets expand into data-sparse regions like the PNW and as climate change intensifies pressure on coastal wetland ecosystems. CO_2 gas flux monitoring requires temporally intensive sampling to capture the effects of cumulative environmental forcings, given the difference between the driving forces in diel versus seasonal timescales. In contrast, CH_4 monitoring requires spatially dense replication to account for microsite heterogeneity. Establishing eddy covariance infrastructure in systems like Kunz Marsh could help integrate and upscale these chamber-based findings into landscape-level net

ecosystem carbon balance estimates, providing the temporal and spatial resolution needed to track salt marsh restoration trajectories over ecologically meaningful timescales.

VI. GENERAL CONCLUSION

The findings of this research reveal that carbon dynamics within Kunz Marsh exhibit a complex relationship with elevation, depending on which aspect of the carbon cycle is examined. Chapter IV found that OM source composition varied systematically with elevation: salt marsh-derived OM dominated throughout the marsh but decreased with elevation, terrestrial contributions increased with elevation, and estuarine contributions remained low throughout but peaked in the low marsh. Despite the elevation-dependent pattern of OM sourcing, Chapter V found that elevation was not a significant driver of CO_2 or CH_4 flux. Instead, CO_2 responded to short-term atmospheric forcings such as PAR and air temperature, whereas CH_4 was governed by finer-scale microsite conditions and plant-mediated transport, as reflected in NDVI being the only significant predictor. This diverging relationship with elevation is informative because it highlights that while elevation structures what carbon enters the system, the eventual fate of that carbon, whether stored or lost as a GHG, appears to be governed by other processes that act independently of the elevation gradient.

The comparison between KH and TMR, the restored and reference high marsh, respectively, adds another important facet to these findings. Despite nearly 30 years of restoration recovery, the restored Kunz high marsh has not converged with the reference high marsh in OM source composition, suggesting that carbon function recovers nonlinearly and that different aspects of the carbon cycle may reach reference-like conditions at different rates. Whether GHG flux dynamics show a similar divergence from reference conditions remains unknown at this site, as pre-restoration flux measurements are lacking, highlighting the importance of establishing baseline flux measurements before restoration wherever possible.

These findings together suggest that long-term, multifaceted monitoring is needed to fully evaluate restoration trajectories.

While Kunz Marsh was a net source of both CO_2 and CH_4 across seasonal sampling dates, and CH_4 emissions expressed in CO_2-equivalent terms during the late-summer diel campaign appeared to substantially exceed GPP at the site, this does not mean that restoration has failed as a climate strategy. Carbon storage in sediments, which was not directly measured here, would need to be incorporated into a full carbon budget before any conclusions about net climate benefit can be drawn. It is also worth noting that the diel campaign may have captured a period of low plant productivity due to late-season senescence, which could partly explain the low GPP estimate. These results emphasize that evaluating restored marshes as climate mitigation tools requires accounting for both the carbon stored and the carbon emitted, and that short-term measurements alone are insufficient to characterize net climate benefit.

Ultimately, this thesis highlights the value of combining OM source characterization with GHG flux measurements to build a more complete picture of carbon dynamics in restored tidal marshes. OM origin reflects carbon inputs to the system, while gas flux captures losses to the atmosphere. As blue carbon markets expand into data-sparse areas like Oregon and as climate change continues to reshape the conditions that influence carbon storage and GHG emissions in tidal marshes, studies that consider these two factors together across restoration gradients and timescales will be increasingly important for ensuring that restored wetland investments deliver genuine climate benefits.

APPENDIX: SUPPLEMENTAL FIGURES AND TABLES

Table S1. GPS coordinates and surface elevations for all flux measurement collars at Kunz Marsh. Collar IDs prefixed with LM, MM, and HM indicate low, mid, and high marsh elevation zones, respectively. Easting and northing are reported in NAD83(2011) / UTM Zone 10N. Elevation is reported in meters relative to NAVD88 using GEOID12B. Coordinates were collected on February 24, 2026, using a Reach RS3 GNSS receiver operating in fixed RTK mode with a base station and rover configuration.

Collar ID	Easting (m)	Northing (m)	Elevation (m NAVD88)	Longitude (°W)	Latitude (°N)
LM1	392919.381	4792907.481	1.866	-124.319769	43.281376
LM2	392937.337	4792922.714	2.155	-124.319551	43.281516
LM3	392910.558	4792922.493	1.861	-124.319881	43.281510
MM1	392962.691	4792857.190	2.464	-124.319226	43.280929
MM2	392947.699	4792911.004	2.330	-124.319421	43.281412
MM3	392929.051	4792903.863	2.362	-124.319649	43.281345
HM1	392959.656	4792820.190	2.724	-124.319256	43.280596
HM2	392973.540	4792818.818	2.753	-124.319084	43.280586
HM3	392990.771	4792818.397	2.725	-124.318872	43.280584
HM4	392945.376	4792814.471	2.733	-124.319431	43.280542
HM5	392980.988	4792810.192	2.754	-124.318991	43.280509

Coordinate system: NAD83(2011) / UTM Zone 10N + NAVD88 (GEOID12B) height. Solution status: Fixed RTK. All measurements collected February 24, 2026.

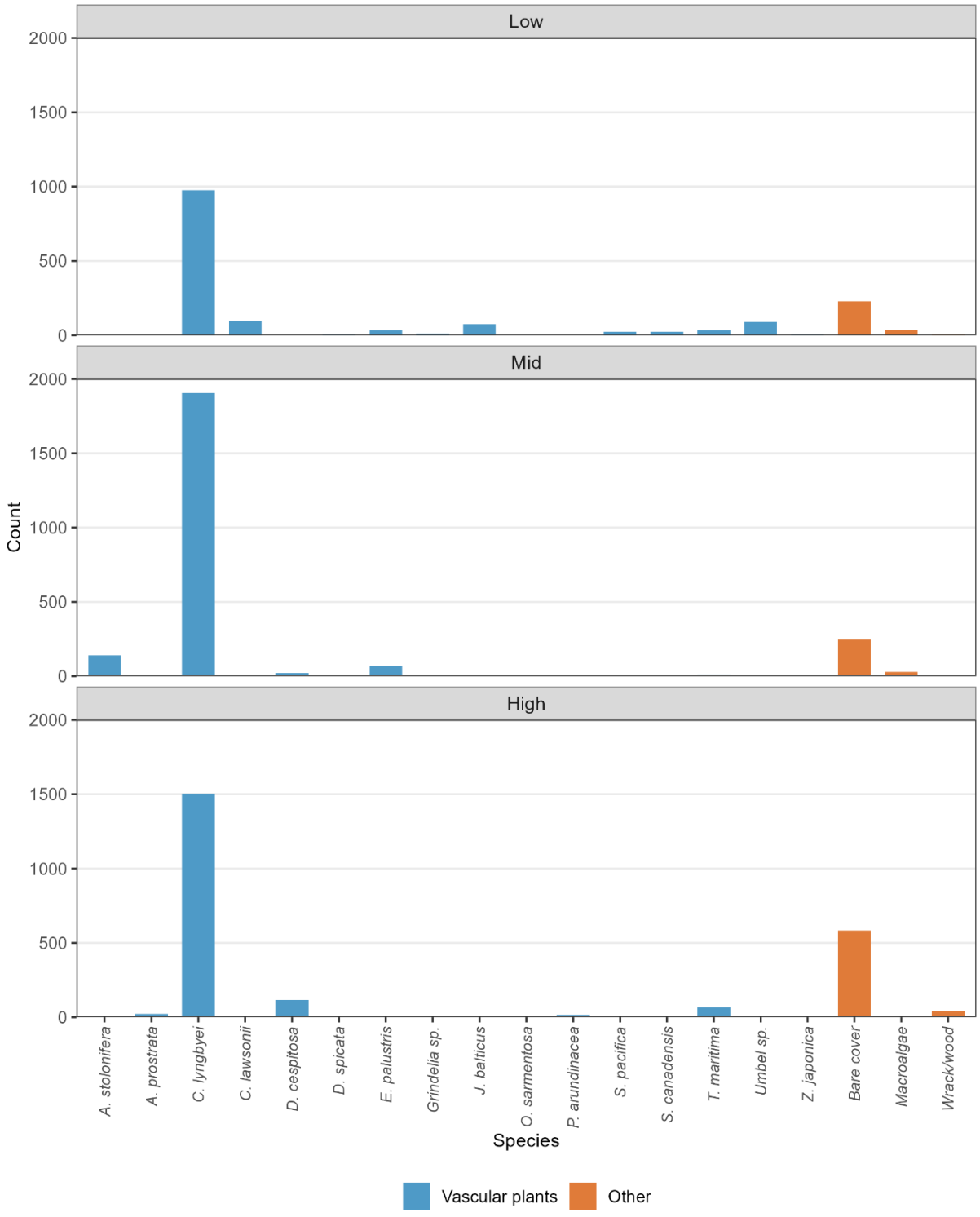


Figure S1. Vegetation composition across low, mid, and high elevation zones at Kunz Marsh based on point-intercept survey data collected by South Slough National Estuarine Research Reserve (SSNERR) staff in 2023. Bars show total point-intercept hit counts for each species, colored by category: vascular plants (blue) and other cover types including bare ground, macroalgae, and wrack or woody debris (orange). *Carex lyngbyei* (C. lyngbyei) was the dominant vascular plant across all elevation zones, with peak abundance in the mid elevation zone.

REFERENCES CITED

Adekanmbi, A. A., X. Shu, Y. Zou, and T. Sizmur. 2022. Legacy effect of constant and diurnally oscillating temperatures on soil respiration and microbial community structure. European Journal of Soil Science 73:e13319.

Arias-Ortiz, A., J. Wolfe, S. D. Bridgham, S. Knox, G. McNicol, B. A. Needelman, J. Shahan, E. J. Stuart-Haëntjens, L. Windham-Myers, P. Y. Oikawa, D. D. Baldocchi, J. S. Caplan, M. Capooci, K. M. Czapla, R. K. Derby, H. L. Diefenderfer, I. Forbrich, G. Groseclose, J. K. Keller, C. Kelley, A. E. Keshta, H. S. Kleiner, K. W. Krauss, R. R. Lane, S. Mack, S. Moseman-Valtierra, T. J. Mozdzer, P. Mueller, S. C. Neubauer, G. Noyce, K. V. R. Schäfer, R. Sanders-DeMott, C. A. Schutte, R. Vargas, N. B. Weston, B. Wilson, J. P. Megonigal, and J. R. Holmquist. 2024. Methane fluxes in tidal marshes of the conterminous United States. Global Change Biology 30:e17462.

Bansal, S., I. F. Creed, B. A. Tangen, S. D. Bridgham, A. R. Desai, K. W. Krauss, S. C. Neubauer, G. B. Noe, D. O. Rosenberry, C. Trettin, K. P. Wickland, S. T. Allen, A. Arias-Ortiz, A. R. Armitage, D. Baldocchi, K. Banerjee, D. Bastviken, P. Berg, M. J. Bogard, A. T. Chow, W. H. Conner, C. Craft, C. Creamer, T. DelSontro, J. A. Duberstein, M. Eagle, M. S. Fennessy, S. A. Finkelstein, M. Göckede, S. Grunwald, M. Halabisky, E. Herbert, M. M. R. Jahangir, O. F. Johnson, M. C. Jones, J. J. Kelleway, S. Knox, K. D. Kroeger, K. A. Kuehn, D. Lobb, A. L. Loder, S. Ma, D. T. Maher, G. McNicol, J. Meier, B. A. Middleton, C. Mills, P. Mistry, A. Mitra, C. Mobilian, A. M. Nahlik, S. Newman, J. L. O'Connell, P. Oikawa, M. P. van der Burg, C. A. Schutte, C. Song, C. L. Stagg, J. Turner, R. Vargas, M. P. Waldrop, M. B. Wallin, Z. A. Wang, E. J. Ward, D. A. Willard, S. Yarwood, and X. Zhu. 2023. Practical guide to measuring wetland carbon pools and fluxes. Wetlands 43:105.

Bellisario, L. M., J. L. Bubier, T. R. Moore, and J. P. Chanton. 1999. Controls on CH_4 emissions from a northern peatland. Global Biogeochemical Cycles 13:81-91.

Brix, H., B. K. Sorrell, and P. T. Orr. 1992. Internal pressurization and convective gas flow in some emergent freshwater macrophytes. Limnology and Oceanography 37:1420-1433.

Brophy, L. S. 2019. Comparing historical losses of forested, scrub-shrub, and emergent tidal wetlands on the Oregon coast, USA: A paradigm shift for estuary restoration and conservation. Report prepared for the Pacific States Marine Fisheries Commission and the Pacific Marine and Estuarine Fish Habitat Partnership. Estuary Technical Group, Institute for Applied Ecology, Corvallis, Oregon.

Cherry, J. A., K. L. McKee, and J. B. Grace. 2009. Elevated CO_2 enhances biological contributions to elevation change in coastal wetlands by offsetting stressors associated with sea-level rise. Journal of Ecology 97:67-77.

Chmura, G. L., S. C. Anisfeld, D. R. Cahoon, and J. C. Lynch. 2003. Global carbon sequestration in tidal, saline wetland soils. Global Biogeochemical Cycles 17:1111.

Chu, H., X. Luo, Z. Ouyang, W. S. Chan, S. Dengel, S. C. Biraud, M. S. Torn, S. Metzger, J. Kumar, M. A. Arain, T. J. Arkebauer, D. Baldocchi, C. Bernacchi, D. Billesbach, T. A. Black, P. D. Blanken, G. Bohrer, R. Bracho, S. Brown, N. A. Brunsell, J. Chen, X. Chen, K. Clark, A. R. Desai, T. Duman, D. Durden, S. Fares, I. Forbrich, J. A. Gamon, C. M. Gough, T. Griffis, M. Helbig, D. Hollinger, E. Humphreys, H. Ikawa, H. Iwata, Y. Ju, J. F. Knowles, S. H. Knox, H. Kobayashi, T. Kolb, B. Law, X. Lee, M. Litvak, H. Liu, J. W. Munger, A. Noormets, K. Novick, S. F. Oberbauer, W. Oechel, P. Oikawa, S. A. Papuga, E. Pendall, P. Prajapati, J. Prueger, W. L. Quinton, A. D. Richardson, E. S. Russell, R. L. Scott, G. Starr, R. Staebler, P. C. Stoy, E. Stuart-Haëntjens, O. Sonnentag, R. C. Sullivan, A. Suyker, M. Ueyama, R. Vargas, J. D. Wood, and D. Zona. 2021. Representativeness of eddy-covariance flux footprints for areas surrounding AmeriFlux sites. Agricultural and Forest Meteorology 301-302:108350.

Colmer, T. D. 2003. Long-distance transport of gases in plants: a perspective on internal aeration and radial oxygen loss from roots. Plant, Cell & Environment 26:17-36.

Comer-Warner, S. A., S. Ullah, W. A. Reyes, S. Krause, and G. L. Chmura. 2022. *Spartina alterniflora* has the highest methane emissions in a St. Lawrence estuary salt marsh. Environmental Research: Ecology 1:011003.

Cornu, C. E., and S. Sadro. 2002. Physical and functional responses to experimental marsh surface elevation manipulation in Coos Bay's South Slough. Restoration Ecology 10:474-486.

Craft, C. 2022. Measuring success: performance standards and trajectories of ecosystem development. Pages 337-367 *in* C. Craft, editor. Creating and restoring wetlands. Second edition. Elsevier, Amsterdam, Netherlands.

Craft, C. B., S. W. Broome, E. D. Seneca, and W. J. Showers. 1988. Estimating sources of soil organic matter in natural and transplanted estuarine marshes using stable isotopes of carbon and nitrogen. Estuarine, Coastal and Shelf Science 26:633-641.

Craven, K. F., R. J. Edwards, and R. P. Flood. 2017. Source organic matter analysis of saltmarsh sediments using SIAR and its application in relative sea-level studies in regions of C4 plant invasion. Boreas 46:642-654.

Drexler, J. Z., M. J. Davis, I. Woo, and S. De La Cruz. 2020. Carbon sources in the sediments of a restoring vs. historically unaltered salt marsh. Estuaries and Coasts 43:1345–1360.

Eidam, E., T. Souza, M. Keogh, D. Sutherland, D. K. Ralston, J. Schmitt, and A. Helms. 2024. Spatial and temporal variability of century-scale sediment accumulation in an active-margin estuary. Estuaries and Coasts 47:2267-2282.

Forbrich, I., and A. E. Giblin. 2015. Marsh-atmosphere CO_2 exchange in a New England salt marsh. Journal of Geophysical Research: Biogeosciences 120:1825-1838.

Frenzel, P., and J. Rudolph. 1998. Methane emission from a wetland plant: the role of CH_4 oxidation in *Eriophorum*. Plant and Soil 202:27-32.

Fritz, C., V. A. Pancotto, J. T. M. Elzenga, E. J. W. Visser, A. P. Grootjans, A. Pol, R. Iturraspe, J. G. M. Roelofs, and A. J. P. Smolders. 2011. Zero methane emission bogs: extreme rhizosphere oxygenation by cushion plants in Patagonia. New Phytologist 190:398-408.

Greiner, J. T., G. M. Wilkinson, K. J. McGlathery, and K. A. Emery. 2016. Sources of sediment carbon sequestered in restored seagrass meadows. Marine Ecology Progress Series 551:95-105.

Hao, Q., Z. Song, X. Zhang, D. He, L. Guo, L. van Zwieten, C. Yu, Y. Wang, W. Wang, Y. Fang, Y. Fang, C.-Q. Liu, and H. Wang. 2024. Organic blue carbon sequestration in vegetated coastal wetlands: Processes and influencing factors. Earth-Science Reviews 255:104853.

Högberg, P. 1997. Tansley Review No. 95 15N natural abundance in soil-plant systems. New Phytologist 137:179-203.

Howe, E. R., and C. A. Simenstad. 2015. Using stable isotopes to discern mechanisms of connectivity in estuarine detritus-based food webs. Marine Ecology Progress Series 518:13-29.

IPCC. 2023. Climate Change 2023: Synthesis Report. Contribution of Working Groups I, II and III to the Sixth Assessment Report of the Intergovernmental Panel on Climate Change. H. Lee and J. Romero, editors. IPCC, Geneva, Switzerland.

Jankowska, E., L. N. Michel, A. Zaborska, and M. Włodarska-Kowalczuk. 2016. Sediment carbon sink in low-density temperate eelgrass meadows (Baltic Sea). Journal of Geophysical Research: Biogeosciences 121:2918-2934.

Janousek, C. N., H. L. Diefenderfer, C. E. Cornu, A. B. Borde, L. S. Brophy, R. M. Thom, and J. K. Apple. 2025a. Local Environmental Drivers of Soil Carbon, Nitrogen, and Organic Matter Decomposition in Pacific Northwest Estuarine Wetlands. Estuaries and Coasts 48:150.

Janousek, C. N., J. R. Krause, J. Z. Drexler, K. J. Buffington, K. L. Poppe, E. Peck, M. F. Adame, E. B. Watson, J. Holmquist, S. D. Bridgham, S. F. Jones, M. Ward, C. A. Brown, L. Beers, M. T. Costa, H. L. Diefenderfer, A. B. Borde, L. Sheehan, J. Rybczyk, C. Prentice, A. B. Gray, A. Hinojosa-Corona, A. C. Ruiz-Fernández, J.-A. Sanchez-Cabeza, K. E. Kohfeld, P. Ezcurra, J. Ochoa-Gómez, K. M. Thorne, M. G. Pellatt, A. M. Ricart, A. M. Nahlik, L. S. Brophy, R. F. Ambrose, M. Lutz, C. Cornu, S. Crooks, L. Windham-Myers, M. Hessing-Lewis, F. T. Short, S. Chastain, T. Williams, T. Douglas, E. Fard, L. Brown, and M. Goman. 2025b. Blue Carbon Stocks Along the Pacific Coast of North America Are Mainly Driven by Local Rather Than Regional Factors. Global Biogeochemical Cycles 39:e2024GB008239.

Kauffman, J. B., L. Giovanonni, J. Kelly, N. Dunstan, A. Borde, H. Diefenderfer, C. Cornu, C. Janousek, J. Apple, and L. Brophy. 2020. Total ecosystem carbon stocks at the marine-terrestrial interface: Blue carbon of the Pacific Northwest Coast, United States. Global Change Biology 26:5679-5692.

Kemp, A. C., C. H. Vane, B. P. Horton, and S. J. Culver. 2010. Stable carbon isotopes as potential sea-level indicators in salt marshes, North Carolina, USA. The Holocene 20:623-636.

Kirwan, M. L., and L. K. Blum. 2011. Enhanced decomposition offsets enhanced productivity and soil carbon accumulation in coastal wetlands responding to climate change. Biogeosciences 8:987-993.

Kirwan, M. L., G. R. Guntenspergen, and J. T. Morris. 2009. Latitudinal trends in *Spartina alterniflora* productivity and the response of coastal marshes to global change. Global Change Biology 15:1982-1989.

Kistritz, R. U., K. J. Hall, and I. Yesaki. 1983. Productivity, detritus flux, and nutrient cycling in a *Carex lyngbyei* tidal marsh. Estuaries 6:227-236.

Langley, J. A., K. L. McKee, D. R. Cahoon, J. A. Cherry, and J. P. Megonigal. 2009. Elevated CO_2 stimulates marsh elevation gain, counterbalancing sea-level rise. Proceedings of the National Academy of Sciences 106:6182-6186.

Lu, W., J. Xiao, F. Liu, Y. Zhang, C. Liu, and G. Lin. 2017. Contrasting ecosystem CO_2 fluxes of inland and coastal wetlands: a meta-analysis of eddy covariance data. Global Change Biology 23:1180-1198.

Mariotti, A., F. Mariotti, M.-L. Champigny, N. Amarger, and A. Moyse. 1982. Nitrogen isotope fractionation associated with nitrate reductase activity and uptake of NO_3^- by Pearl Millet. Plant Physiology 69:880-884.

Mitra, B., G. Miao, K. Minick, S. G. McNulty, G. Sun, M. Gavazzi, J. S. King, and A. Noormets. 2019. Disentangling the effects of temperature, moisture, and substrate availability on soil CO_2 efflux. Journal of Geophysical Research: Biogeosciences 124:2060-2075.

Mitrovic, S. M., and D. S. Baldwin. 2016. Allochthonous dissolved organic carbon in river, lake and coastal systems: transport, function and ecological role. Marine and Freshwater Research 67:i-iv.

Morin, T. H., G. Bohrer, K. C. Stefanik, A. C. Rey-Sanchez, A. M. Matheny, and W. J. Mitsch. 2017. Combining eddy-covariance and chamber measurements to determine the methane budget from a small, heterogeneous urban floodplain wetland park. Agricultural and Forest Meteorology 237:160-170.

Moseman-Valtierra, S., O. I. Abdul-Aziz, J. Tang, K. S. Ishtiaq, K. Morkeski, J. Mora, R. K. Quinn, R. M. Martin, K. Egan, E. Q. Brannon, J. Carey, and K. D. Kroeger. 2016. Carbon dioxide fluxes reflect plant zonation and belowground biomass in a coastal marsh. Ecosphere 7:e01560.

Niu, S., W. Chen, L. L. Liáng, C. A. Sierra, J. Xia, S. Wang, M. Heskel, K. F. Patel, B. Bond-Lamberty, J. Wang, G. Yvon-Durocher, M. U. F. Kirschbaum, O. K. Atkin, Y. Huang, G. Yu, and Y. Luo. 2024. Temperature responses of ecosystem respiration. Nature Reviews Earth & Environment 5:559-571.

Noyce, G. L., and J. P. Megonigal. 2021. Biogeochemical and plant trait mechanisms drive enhanced methane emissions in response to whole-ecosystem warming. Biogeosciences 18:2449-2463.

O'Connor, J. J., B. J. Fest, M. Sievers, and S. E. Swearer. 2019. Impacts of land management practices on blue carbon stocks and greenhouse gas fluxes in coastal ecosystems—A meta-analysis. Global Change Biology 26:1354-1366.

Peck, E. K., M. Goñi, and R. A. Wheatcroft. 2025. Spatiotemporal controls on organic matter sourcing to minerogenic salt marshes. Limnology and Oceanography 70:84-99.

Peterson, B. J., R. W. Howarth, and R. H. Garritt. 1985. Multiple stable isotopes used to trace the flow of organic matter in estuarine food webs. Science 227:1361-1363.

Ratliff, K. M., A. E. Braswell, and M. Marani. 2015. Spatial response of coastal marshes to increased atmospheric CO_2. Proceedings of the National Academy of Sciences 112:15580-15584.

Ruiz-Plancarte, J., J. D. Fuentes, and K. J. McGlathery. 2026. Controls on seasonal atmosphere-ecosystem carbon dioxide exchanges in a temperate salt marsh. Global Change Biology 32:e70740.

Sage, R. F., and D. S. Kubien. 2007. The temperature response of C3 and C4 photosynthesis. Plant, Cell & Environment 30:1086-1106.

Schultz, M. A., C. N. Janousek, L. S. Brophy, J. Schmitt, and S. D. Bridgham. 2023. How management interacts with environmental drivers to control greenhouse gas fluxes from Pacific Northwest coastal wetlands. Biogeochemistry 165:165-190.

Sculthorpe, C. D. 1967. The biology of aquatic vascular plants. Edward Arnold, London. 610 pp.

Shahan, J., H. Chu, L. Windham-Myers, M. Matsumura, J. Carlin, E. Eichelmann, E. Stuart-Haentjens, B. Bergamaschi, K. Nakatsuka, C. Sturtevant, and P. Oikawa. 2022. Combining eddy covariance and chamber methods to better constrain CO_2 and CH_4 fluxes across a heterogeneous restored tidal wetland. Journal of Geophysical Research: Biogeosciences 127:e2022JG007112.

Stock, B. C., A. L. Jackson, E. J. Ward, A. C. Parnell, D. L. Phillips, and B. X. Semmens. 2018. Analyzing mixing systems using a new generation of Bayesian tracer mixing models. PeerJ 6:e5096.

Turner, K. E. 1996. Field measurements of methane efflux and laboratory measurements of resistance to passive methane transport through *Carex lyngbyaei*. M.S. thesis. University of Alaska Anchorage, Anchorage, Alaska, USA.

Verville, J. H., S. E. Hobbie, F. S. Chapin, and D. U. Hooper. 1998. Response of tundra CH_4 and CO_2 flux to manipulation of temperature and vegetation. Biogeochemistry 41:215-235.

Waldo, N. B., B. K. Hunt, E. C. Fadely, J. J. Moran, and R. B. Neumann. 2019. Plant root exudates increase methane emissions through direct and indirect pathways. Biogeochemistry 145:213-234.

Ward, M. A., T. M. Hill, C. Souza, T. Filipczyk, A. M. Ricart, S. Merolla, L. R. Capece, B. C. O'Donnell, K. Elsmore, W. C. Oechel, and K. M. Beheshti. 2021. Blue carbon stocks and exchanges along the California coast. Biogeosciences 18:4717-4732.

Whiting, G. J., and J. P. Chanton. 1992. Plant-dependent CH_4 emission in a subarctic Canadian fen. Global Biogeochemical Cycles 6:225-231.

Williams, T., C. N. Janousek, M. A. McKeon, H. L. Diefenderfer, C. E. Cornu, A. B. Borde, J. Apple, L. S. Brophy, M. Norwood, M. A. Schultz, and S. D. Bridgham. 2025. Methane and nitrous oxide fluxes from reference, restored, and disturbed estuarine wetlands in Pacific Northwest, USA. Ecological Applications 35:e70011.

Wimalasekera, R. 2019. Effect of light intensity on photosynthesis. Pages 65-73 Photosynthesis, Productivity and Environmental Stress. John Wiley & Sons, Ltd.

Zhang, J., Q. Hao, Q. Li, X. Zhao, X. Fu, W. Wang, D. He, Y. Li, Z. Zhang, X. Zhang, and Z. Song. 2024. Source identification of sedimentary organic carbon in coastal wetlands of the western Bohai Sea. Science of the Total Environment 913:169282.